GENERAL ATOMIC

DIVISION OF GENERAL DYNAMICS

AEC RESEARCH AND
DEVELOPMENT REPORT

GA-6583

DIFFERENTIAL NEUTRON THERMALIZATION

by

W. L. Whittemore

ANNUAL SUMMARY REPORT
October 1, 1964 through September 30, 1965

Contract AT(04-3)-167
Project Agreement No. 10
U. S. Atomic Energy Commission

December 2, 1965

DISCLAIMER

GENERAL ATOMIC

DIVISION OF

GENERAL DYNAMICS

JOHN JAY HOPKINS LABORATORY FOR PURE AND APPLIED SCIENCE

P.O. BOX 608, SAN DIEGO, CALIFORNIA 92112

GA-6583

DIFFERENTIAL NEUTRON THERMALIZATION

ANNUAL SUMMARY REPORT
October 1, 1964 through September 30, 1965

Work Done by:

S. Boehm
A. K. Hom
D. Parks
G. Rothbart
W. L. Whittemore

Report written by:

W. L. Whittemore

Contract AT(04-3)-167
Project Agreement No. 10
U. S. Atomic Energy Commission
General Atomic Project No. 220

December 2, 1965

PREVIOUS REPORTS IN THIS SERIES

GA-2503	Annual Summary Report October 1, 1960 - September 30, 1961
GA-3409	Annual Summary Report October 1, 1961 - September 30, 1962
GA-4434	Annual Summary Report October 1, 1962 - September 30, 1963
GA-5554	Annual Summary Report October 1, 1963 - September 30, 1964

FOREWORD

This annual summary report was prepared by General Dynamics/ General Atomic Division, San Diego, California, on USAEC contract AT(04-3)-167, Project Agreement No. 10, titled "Differential Neutron Thermalization." Dr. W. L. Whittemore is the General Atomic principal investigator on this project.

This report covers research conducted during the period of October 1, 1964 through September 30, 1965. The General Atomic project number is 220.

ABSTRACT

The General Atomic Neutron Velocity Selector has been exploited during the present contract year for the study of the inelastic scattering of monoenergetic neutrons in a variety of materials. The scattering into various angular directions between 30 deg and 150 deg has been studied for incident neutrons with energies up to 0.6 eV. Because of the ability of this apparatus to study details of single scattering events with neutrons which have energies significantly higher than are available with reactor-based experiments, most of the present work was done for $E_o > 0.20$ eV. The exact incident energy was chosen to optimize the ability to study various chemical rotation and vibration levels in this higher energy region. Additional technical details of the experimental apparatus are discussed in Section 2. Numerous details are given in Sections 3 through 6 for neutron interactions in polyethylene, methane, graphite and hydrides of rare earth metals. In most cases, theoretical results are compared in detail with experimental results.

THIS PAGE

WAS INTENTIONALLY

LEFT BLANK

CONTENTS

THIS PAGE

WAS INTENTIONALLY

LEFT BLANK

FIGURES

FIGURES (Cont.)

FIGURES (Cont.)

1. INTRODUCTION

The experimental and theoretical work carried out during this reporting period has continued the fundamental studies of the interaction mechanisms by which neutrons exchange energy with moderating materials. This program is concerned with the basic interactions of a neutron with thermal, molecular, and crystal vibrations or rotations. It includes:

a. Experimental determination of the interaction cross sections and the angular and energy distribution for neutrons after single scattering events in various media, and determination of the scattering cross section and of the Scattering Law;

b. Theoretical interpretations of the experimental data, aimed at making the results available in a form useful either to reactor designers or to reactor physicists interested in fundamental interactions between neutrons and moderating materials.

In this report, the results of the current year's work are presented. The experimental techniques were discussed in some detail in earlier reports.[1-4] Additional details for using the neutron velocity selector to derive accurate quantitative differential cross sections are discussed in Section 2. In subsequent sections, experimental results are presented and discussed.

One of the objects of immediate concern is the binding of hydrogen in numerous materials ranging from liquid methane through polymerized hydrocarbons (such as polyethylene) to metal hydrides. The other concern is with neutron interactions with non-hydrogen moderators such as graphite. The problems of binding in these materials are neither simple nor consistent. The rotational and vibrational modes in liquid methene interact with neutrons quite differently than do those in the long, linear chain molecules in polyethylene or in the vibrational levels (some sharp, some diffuse) in the metal hydrides. In the following treatments, the appropriate theory is compared with the experimental results in an effort to verify the theory for use in reactor thermalization applications.

THIS PAGE

WAS INTENTIONALLY

LEFT BLANK

2. EXPERIMENTAL TECHNIQUES

The experimental arrangement used to study neutron inelastic scattering with an electron linear accelerator (Linac) has been discussed in considerable detail in earlier reports.[1-4] Some improvements and additional considerations treated this year are included below.

2.1 Data Reduction and the Computer Code-CROSEC

Although the measurement of the scattering cross section $\sigma(E_o, E, \theta)$, in units of barns steradian per electron-volt per molecule of scattering material, has been treated earlier,[4] it is outlined below for the convenience of the reader. The scattering cross section from vanadium, used as a standard, is well known to be incoherent and elastic, with the scattered neutron energy very nearly equal to the ingoing incident energy. When this comparison technique is used in its simplest form to evaluate the scattering from an hydrogenous moderator material, the major complication is the treatment of the absorption cross section in the vanadium. Usual hydrogen moderating materials have a nearly vanishing absorption cross section. The technique described in this section treats the sample scattering in the single scattering approximation, which is extremely good for all of the studies made to date, since all scattering samples have been very "thin", with a total transmission of $\gtrsim 0.9$ for the incident neutron beam in the scattering position. Appropriate multiple-scattering corrections are being evaluated at this writing but are not yet available.

In the following discussion, we derive the basic formulation of the scattering from thin samples used to the present work. Let subscript v refer to the vanadium standard and subscript s refer to any sample whose scattering is under consideration. The following definitions and assumptions underly this derivation:

σ_T, $\sigma_{T'}$ = total neutron cross sections for the scattering material before and after the single scattering event.

$\sigma_T = \sigma_a + \sigma_s$, $\sigma_{T'} = \sigma_{a'} + \sigma_{s'}$, the absorption and scattering cross sections.

Area of vanadium standard = area of sample.

$(d\sigma_s/d\Omega)_v = (\sigma_s)_v/4\pi$.

$(\sigma_T)_v = 5.09 + 5.29\,(0.025/E)^{\frac{1}{2}}$, where E is neutron energy in eV.

θ_i = angle less than 90 degrees between the normal to the scattering sample and the incident neutron direction.

θ_o = neutron outgoing angle after scattering, measured with respect to the normal to the surface of the scattering plane; the normal is chosen on the side of the plane from which the neutron emerges.

θ_j = neutron scattering angle measured with respect to the incident neutron direction.

$N_s(E_o, E, \theta_j)\Omega$ and $N_v(E_o, E, \theta_j)\Omega$ = the number of neutrons scattered in the laboratory system in a solid angle Ω about θ_j from the sample and from vanadium, respectively, for the same number N_o of neutrons incident on the scattering sample.

n = number of scattering centers per cm^3 of scattering material.

R = linear thickness of the scattering sample measured normal to its surface.

Using elementary integral calculus techniques, one can show that the number of neutrons incident on the scatterer with energy E_o, which undergo single scattering and emerge in a solid angle Ω about an angle θ_j, with final energy E, is given as follows:

With scatterer in <u>transmission</u> position, and for $0 \leq \theta_j \leq 90$ deg,

$$N(E_o, E, \theta_j)\Omega = \frac{N_o nR}{\cos\theta_i}\left(\frac{d^2\sigma_s}{dEd\Omega} \times \Omega\right) e^{-\frac{n\sigma'_a R}{\cos\theta_o}} \left[\frac{1-e^{-nR\left(\frac{\sigma_T}{\cos\theta_i} - \frac{\sigma'_a}{\cos\theta_o}\right)}}{nR\left(\frac{\sigma_T}{\cos\theta_i} - \frac{\sigma'_a}{\cos\theta_o}\right)}\right] \quad ; \quad (1a)$$

With scatterer in reflection position, and for $90 \leq \theta_j \leq 180$ deg,

$$N(E_o, E, \theta_j)\Omega = \frac{N_o nR}{\cos\theta_i}\left(\frac{d^2\sigma_s}{dEd\Omega} \times \Omega\right)\left[\frac{1 - e^{-nR\left(\frac{\sigma_T}{\cos\theta_i} + \frac{\sigma'_a}{\cos\theta_o}\right)}}{nR\left(\frac{\sigma_T}{\cos\theta_i} + \frac{\sigma'_a}{\cos\theta_o}\right)}\right] . \qquad (1b)$$

This formulation is for vanadium and any other scattering sample which has a non-vanishing absorption cross section. It provides for full attenuation of the incident beam prior to the single scattering event and allows for absorption of the scattered beam. Attenuation of the scattered beam by scattering is not allowed in the single scattering approximation. In the case of scattering from vanadium, equations (1a) and (1b) simplify somewhat by virtue of the fact that $E_o = E$ and $(d^2\sigma/dEd\Omega)v = 0$ when $E_o \neq E$. For a scattering sample with negligible absorption cross section ($\sigma_a \approx 0$), such as for most hydrogenous moderators, the above formulae reduce as follows:

$$N(E_o, E, \theta_j)\Omega = \frac{N_o nR}{\cos\theta_i}\left(\frac{d^2\sigma_s}{dEd\Omega} \times \Omega\right)\left[\frac{1 - e^{-nR\sigma_s/\cos\theta_i}}{nR\sigma_s/\cos\theta_i}\right] . \qquad (2)$$

The inclusion of the scattering cross section for the outgoing beam attenuation would be an error because this would effectively permit more than one scattering, which violates the basic hypothesis of single scattering. Moreover, an inclusion of the scattering cross section for the outgoing neutrons would make an error of the same magnitude as that caused by multiple scattering, but in the wrong direction. Kottwitz et al[5] have shown that a specimen of vanadium 0.25-in. thick requires considerable multiple scattering correction. This correction is due mainly to the absorption in the vanadium and is apparently caused by the fact that multiple scattering effectively increases the pathlength of a neutron prior to its emergence from the scattering sample. Due to absorption, the longer effective pathlength reduces the intensity. Kottwitz has made a transport calculation for this case. In the scattering experiments currently underway at General Atomic, the scattering thickness of vanadium is less than 1/3 that used by Kottwitz. The effect of the multiple scattering will be considerably less in this case and, for the present, has not been included

in the current calculations. It is perhaps interesting to note that if the total cross section for vanadium were due only to scattering, then the effects of multiple scattering would be negligible, regardless of thickness of scattering samples, so long as the scattering cross section were precisely isotropic. The reason for this is that regardless of thickness and in the absence of absorption, all neutrons incident from a well-collimated direction emerge with a completely isotropic distribution after every scattering, regardless of the number of scattering events.

During this contract year, a computer program has been written to process the raw data from the neutron scattering experiments. This program (called CROSEC) performs the necessary calculations on the data to yield the scattering cross section $\sigma(E_o, E, \theta)$, the differential cross section $d\sigma/\sigma\Omega$, and the Scattering Law $S(\alpha, \beta)/\alpha$. A subroutine TPLOT[6] has been incorporated into CROSEC and, in conjunction with the SC 4020 plotter, provides graphs of the scattering kernel as a function of final energy and $S(\alpha, \beta)/\alpha$ as a function of β. Use of this program CROSEC has proved to be highly beneficial and troublefree.

The number of neutron counts in each time channel is punched out on paper punch tape by the multi-channel analyzer. This punch tape and the standard data sheets are then turned in at the computer department for conversion to IBM cards, which are submitted with the program for processing on the IBM 7044. This program greatly simplifies the work involved in analyzing the experimental data by dispensing with the large number of hand calculations previously necessary. In addition, the pertinent quantities are available in plotted form a day or so after the experimental run, much sooner than previously possible with hand computations.

2.1.1 Data input

For each particular incident neutron energy and a particular scattering angle, a small deck of data cards is required. Eleven of the cards are the same for each job and contain such information as labels for the graphs, distances to the various detectors, and parameters describing the vanadium standard: thickness, area, scattering cross section, etc. All these quantities are the same for each job, but flexibility is provided by making them part of the data input. If at some future time changes were made, i.e., a standard scatterer other than vanadium were used, the appropriate changes could be made on these data cards without the necessity of changing the program itself.

Other data are required for each job identifying it as to date, incident neutron energy, scattering angle, and orientation of the scatterer. Additional data are required indicating the kind of detector located at this particular angle, so that a correction can be made for the efficiency of the detector, and describing the scattering sample by giving its thickness,

area, scattering, and absorption cross sections, effective mass, etc. The normalization factors for the background, aluminum holder, and vanadium standard must be given. The actual number of neutron counts per time channel for the signal, background aluminum holder, its background, the vanadium holder, and its background must also be given; but most of this data is punched on paper tape and is easily converted to IBM cards.

2.1.2 Calculations and output

CROSEC first prints out all the input data. This serves to identify the calculation and acts as a check for possible errors in data input. The series of calculations which are then carried out are listed below progressively:

1. The background is averaged five channels at a time to smooth out the fluctuations. It is then normalized and printed out.
2. This background is subtracted from the signal and the result is printed out.
3. The net aluminum is calculated (aluminum minus its background) and subtracted from the net signal above. The result is printed out.
4. The subroutine TPLOT is called, and plots of net signal (signal minus background) and net aluminum are made on the same graph, as a function of time channel.
5. The net vanadium (vanadium minus its background) is calculated and printed out.
6. The energy is calculated as a function of channel number.
7. The correction factor for detector efficiency is calculated as a function of channel number.
8. The corrected signal [(signal minus background minus net aluminum) times correction factor] is calculated as a function of time channel.
9. The results of calculations 3, 5, 6, 7, and 8 are printed out together as a function of channel number.
10. The corrected signal and corrected vanadium (net vanadium times correction factor) are summed over all channels, and the vanadium total is multiplied by the vanadium normalization factor. These two results are printed out.
11. A subroutine SIGMA is called, and the differential cross section is calculated.

12. The scattering kernel is calculated as a function of final energy, and the result is printed out.

13. The TPLOT subroutine is again called, and a plot is made of kernel versus final energy.

14. $\beta = (E_f - E_o)/kT$ is calculated as a function of time channel.

15. $\alpha = (E_f + E_o - 2 E_o E_f \cos\theta)/MkT$ is calculated as a function of time channel.

16. $S(\alpha, \beta)$ and $S(\alpha, \beta)/\alpha$ are calculated and printed out along with α, β, and the scattering kernel, as a function of final energy.

17. The TPLOT subroutine is called, and a plot is made of ALPHA versus BETA.

18. TPLOT is again called, and a plot is made of $S(\alpha, \beta)/\alpha$ versus β.

19. The differential cross section is printed out.

20. A check is made to see if there is another job to be calculated. If so, control is transferred to an early part of the program, and all the above calculations are made for the next job in the series. When the last job is finished, a final call to TPLOT is made which rewinds the tape on which all the plotting instructions have been written, and the program ends.

2.2 Multiple Scattering Effects

As of this writing, multiple scattering corrections have not been evaluated theoretically for the cases studied experimentally in this program. Work is under way at present to apply the corrections derived in another program to the problems studied in this program. First results of a complete theoretical study on water have indicated that for "thin" (transmission ~0.85) samples, many of the energy transfers require corrections which are less than 10 percent. These cases involve outgoing neutrons which have scattering cross sections substantially unchanged from that of the incident neutron. Multiple scattering corrections in a specimen with substantial absorption cross section are different from those in a specimen which predominantly scatters. Kottwitz[5] has treated vanadium, which is such a case.

The present program has undertaken to evaluate roughly the magnitude of the effect of multiple scattering by measuring the differential cross section for two thicknesses. In the case of polyethylene, these two thicknesses were chosen to give transmissions of about 0.80 and 0.90. For zirconium hydride, the thicknesses gave transmissions of 0.85 and 0.92.

As will appear below (Section 3.2), the multiple scattering in polyethylene is small (5 to 10 percent) for most energy transfers except for those with very small final energies where the scattering cross section is very much increased. For zirconium hydride, the two thicknesses used revealed no change in the indicated width of the energy level at 0.14 eV. One concludes that for the circumstances of this experiment (E_o = 0.24 eV and E = 0.10 eV), the multiple scattering corrections are small as expected, since the scattering cross sections did not change significantly during the scattering event.

In the considerations of multiple scattering effects, it can be a happy result that the required corrections may be smaller for double differential cross sections than for some of the single differential cross sections. Such a state of affairs may pertain for "thin" samples if the incident energy E_o is large (compared with 0.025 eV), and final energies which are low enough to give substantially increased scattering cross sections are not considered. Double differential measurements allow one to ignore those scattered neutrons with very low energy for which large corrections are required. Single differential measurements made with a technique which detects all scattered neutrons at a given scattering angle without distinguishing the final energies must, of necessity, require particular corrections for the very low energy scattered neutrons.

2.3 Instrument Performance

The performance of the General Atomic Neutron Velocity Selector used in conjunction with the Linac to study neutron inelastic scattering experiments will be discussed in this section. Particular attention will be given to the energy resolution of the apparatus. The beam size of the system at the position of the scattering sample is 7.0 cm by 25.4 cm, or about 178 cm^2. Of course, smaller sample sizes can be utilized as beam intensity permits. The beam intensity depends on the incident energy selected but is in the range 5 to 7 x 10^5 neutrons/min for incident energies in the range 0.15 to 0.5 eV. This intensity is obtained with an average beam power of about 11 kW, using a tungsten electron-neutron converter and a neutron source moderator of about 1.5-in thickness. Reference to Figure 1 will make the geometrical layout clearer.

Much of the recent operation has been performed with the chopper described earlier, [1-3] using a new chopper slit system. For the work performed this contract year, the chopper was rotated at a speed of 180 rps. This speed and the attendant experimental arrangement gave the resolutions summarized in Table I, where

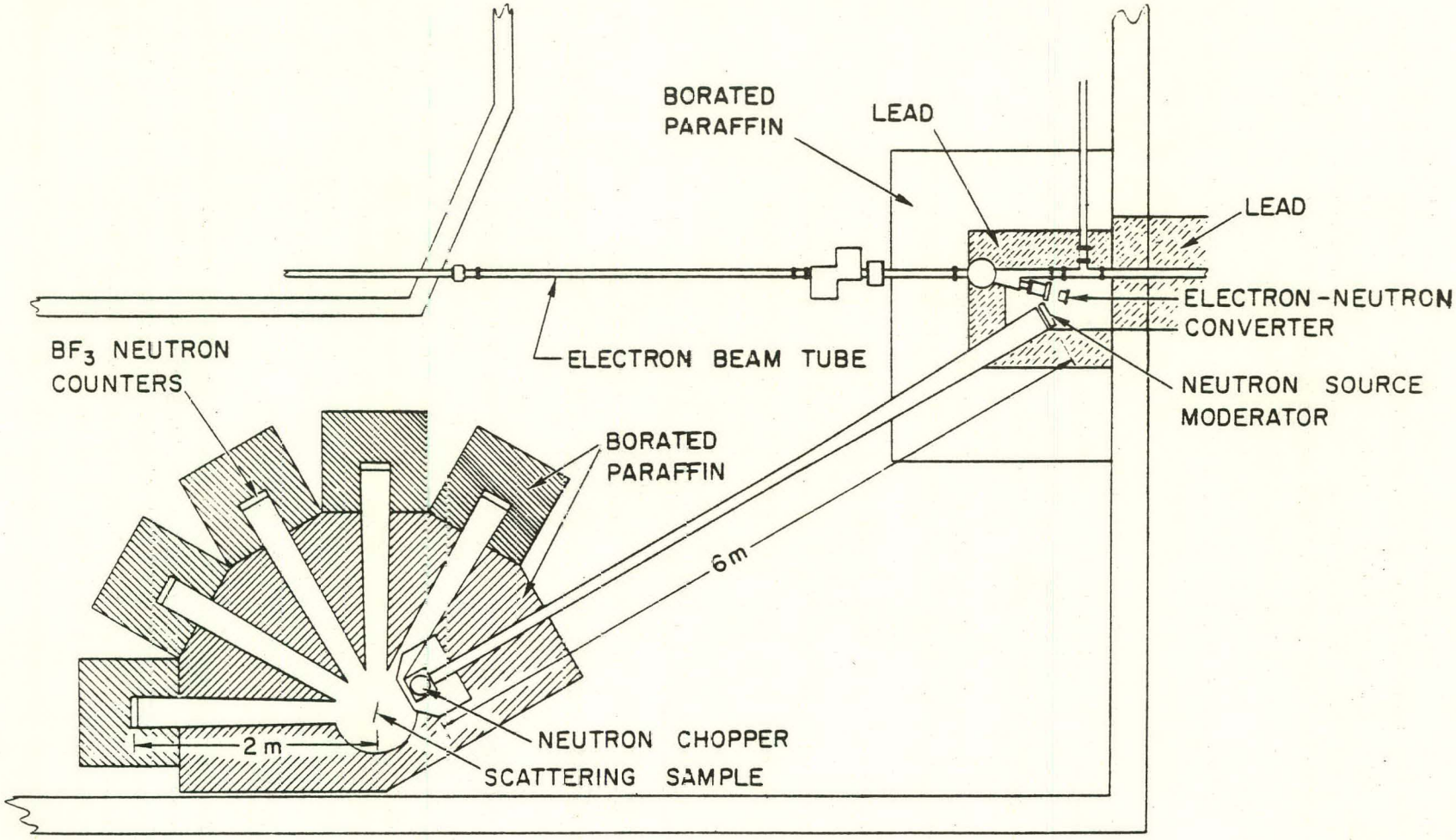

Fig. 1--Experimental arrangement for General Atomic Neutron Velocity Selector and scattering apparatus, used in conjunction with Electron Linear Accelerator

E_o is the incident energy

E is the final energy,

$\epsilon = E_o - E$ = energy transfer,

ΔE_o is the distribution in incident energy,

$(\Delta E)_{calc}$ is the calculated final energy resolution.

TABLE I

Typical Calculated Energy Resolution $(\Delta E)_{calc}$ in Final Energy E as a Function of Incident Energy E_o and Energy Transfer ϵ

E_o (eV)	ϵ (eV)	E (eV)	$(\Delta E)_{calc}$ (eV)	ΔE_o [a] (eV)
0.167	0.100	0.067	0.018	0.0093
0.233	0.150	0.083	0.029	0.016
0.408	0.200	0.208	0.083	0.036
0.499	0.360	0.139	0.076	0.049

[a] The spread in incident energy ΔE_o is due to the chopper-open time and the source-emission time.

A computer program evaluates $(\Delta E)_{calc}$ for the experimental conditions and includes the effect of a) duration of the neutron source pulse, b) chopper "open" time, c) various flight paths, d) energy loss ϵ in scatterer, and e) width of energy level. When the width of the energy level giving rise to the energy transfer ϵ is taken as zero, the width $(\Delta E)_{calc}$ gives the resolution of the apparatus. In other words, an energy level of zero width giving rise to an energy transfer ϵ will have an apparent width $(\Delta E)_{calc}$.

2.4 Upgrading Capability

In addition to planned improvements to the General Atomic Linac, which are expected to increase the neutron output for the present experiment by a factor of 2-4 in the near future, improved capabilities of the Neutron Velocity Selector are being implemented. In the near future, the rotational speed of the chopper will be increased to 240 rps, at which

time the chopper "open" time t will be decreased to ~14 μsec. The improved resolution is illustrated in Table II where the half width τ and Δt_o are for pulses measured just behind the chopper and at the detector for neutrons with energy E_o. $(\Delta E)_{calc}$ is the calculated resolution for inelastic scattering.

TABLE II

Summary of Resolution with a Chopper

E_o(eV)	ΔE_o(eV)	τ(μsec)	Δt_o(μsec)	E_f(eV)	ϵ(eV)	$(\Delta E)_{calc}$(eV)
0.167	0.0067	14	19	0.067	0.100	0.014
0.233	0.011	14	19	0.100	0.133	0.025
0.410	0.026	14	19	0.100	0.310	0.039

Although the present thrust ball bearings are likely to work satisfactorily, some attention has been given to an alternative support system using air bearings. Figures 2 to 4 show a mockup system using a lower thrust airbearing and an upper sleeve airbearing. The body of the rotating member duplicated the chopper in use (14 inches long, 6 inches diameter and 50 pounds weight). An air pressure of 80 psi applied to these bearings, which were designed to give radial clearances of ~0.015 in. and bottom clearance of -0.015 in., gave good promise of operation. The existing thrust bearing presented too small a support area by about a factor of 2 to 4. The tests conducted so far, at speeds up to 2100 RPM, have given results which show the way to design a satisfactory thrust airbearing for the present application.

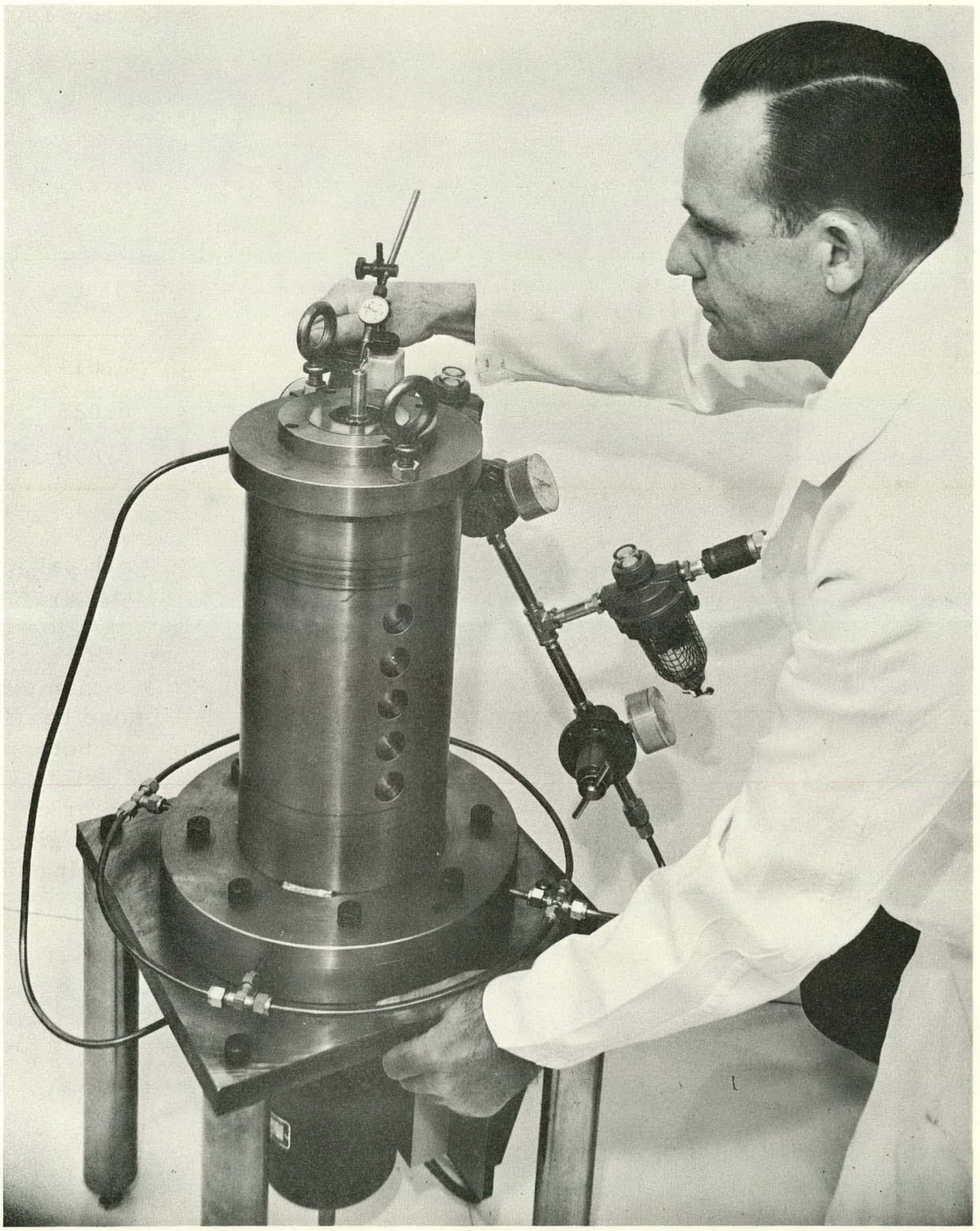

Fig. 2--Fully assembled chopper with upper and lower airbearings

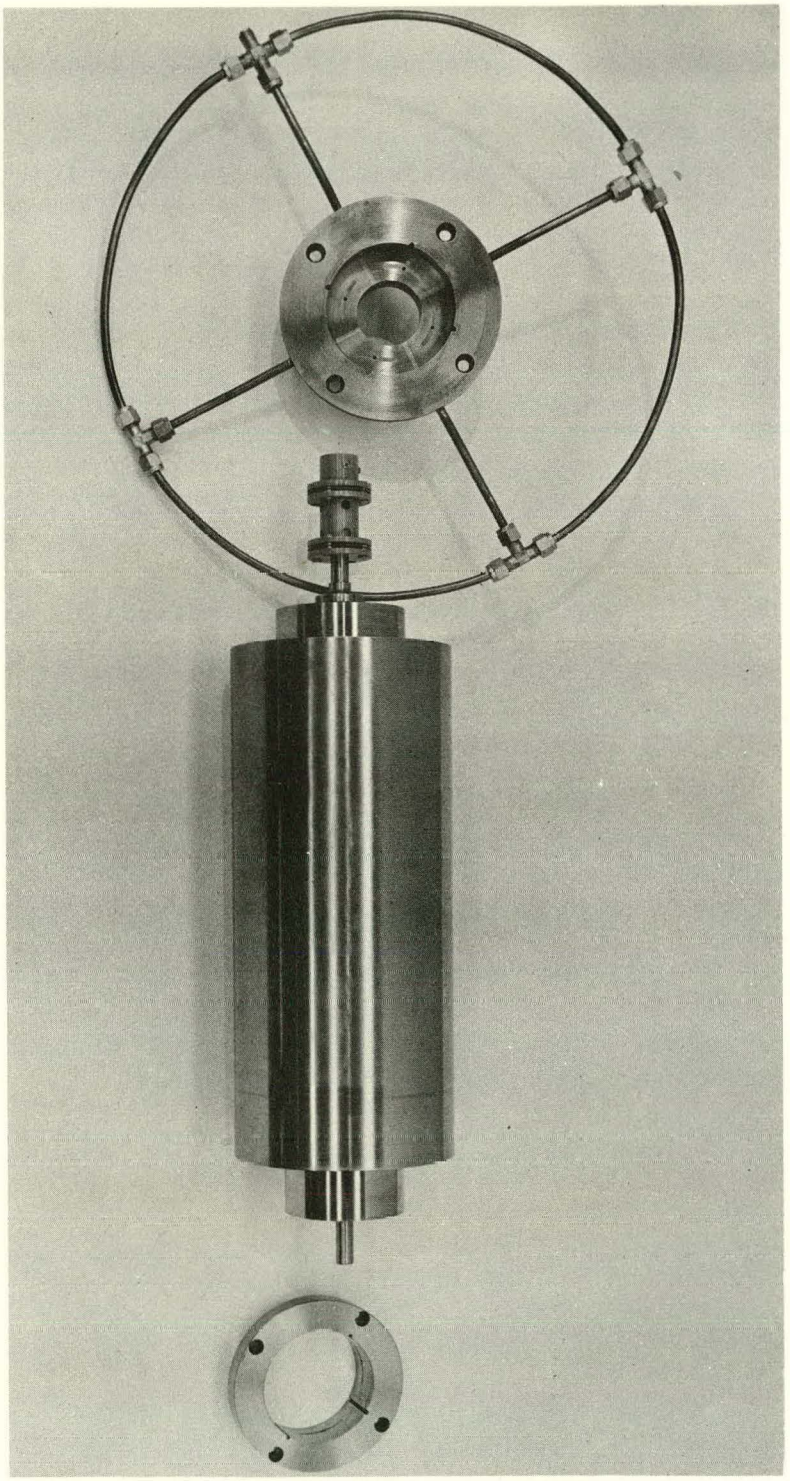

Fig. 3--An exploded view of the chopper rotor, showing the details of the upper and lower airbearings. Note that the rotor duplicates the chopper rotor in mass but does not have the chopper inserts.

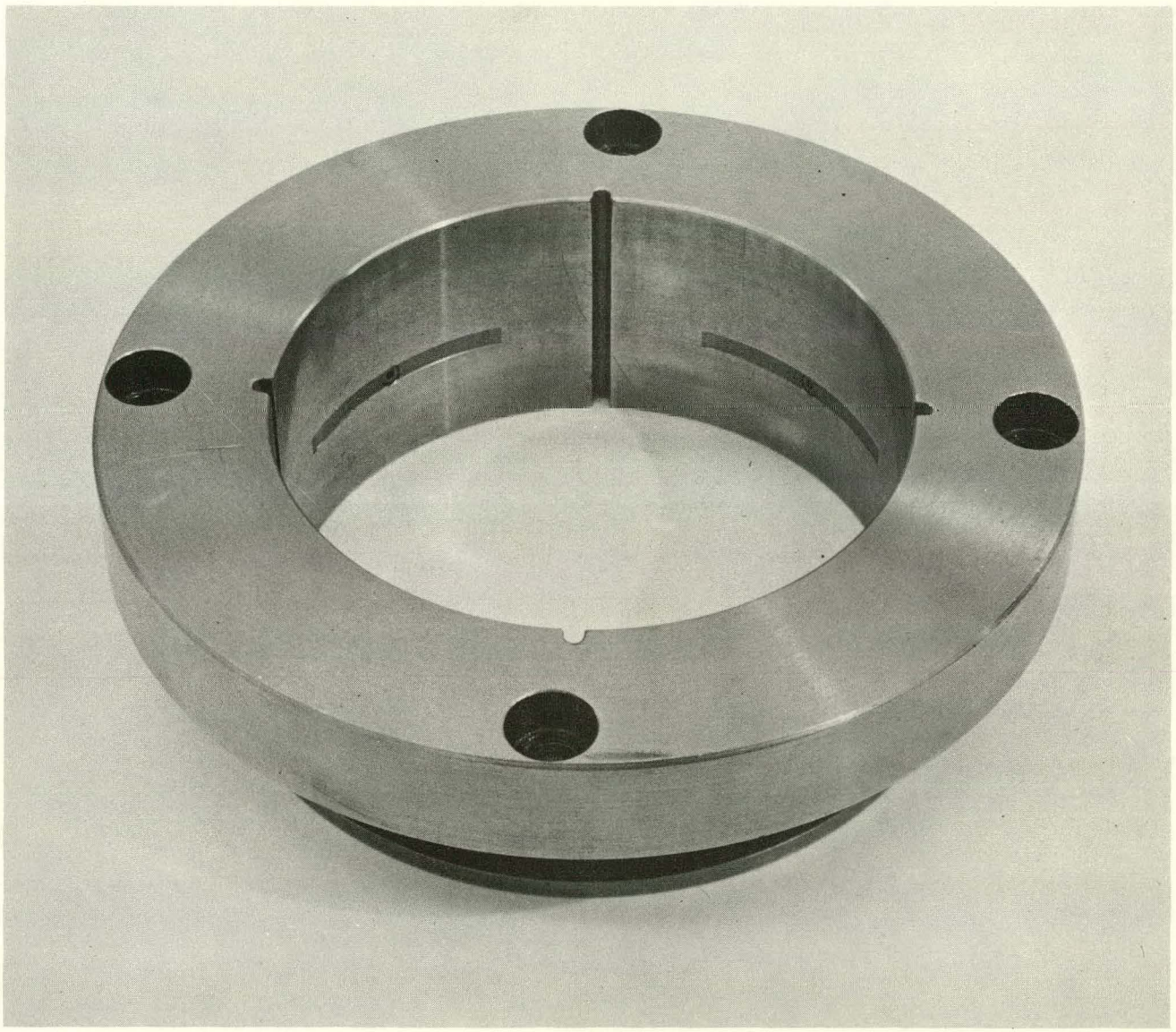

Fig. 4--Details of the chopper airbearing

THIS PAGE

WAS INTENTIONALLY

LEFT BLANK

3. NEUTRON SCATTERING BY POLYETHYLENE

A great deal of study has been devoted to hydrogenous scattering systems, with special reference to their pertinence to neutron thermalization. Light water, in particular, has received much attention, both theoretical and experimental. Neutron interactions in polyethylene have come under investigation somewhat more recently. Among the first theoretical treatments of neutron scattering in polyethylene were those of Goldman and Federighi[7] and Parks[8]. Parks developed a method of computing the scattering cross section from a rather realistic, distributed frequency spectrum. Goldman has suggested that the frequency distribution for the long chain molecules be represented by five Einstein frequencies, in a method analogous to that used by Nelkin[9] for water. More recently Koppel and Young[10] have further refined the technique, using isolated Einstein frequencies. In a separate program oriented toward developing an understanding of the organic moderators, McMurry* has developed a scattering cross section for n-butane, in which a contribution by CH_2 radicals is a significant component.

A large portion of the attendent analysis will be based on the differential scattering cross section $\sigma(E_o, E, \theta)$ rather than the Scattering Law representation of the data. Although higher phonon terms limit the significance of the frequency distribution derived from the extrapolation procedure, use of the Scattering Law representation provides a highly beneficial check on interconsistency of the data.

3.1 Experimental Procedure

The General Atomic Neutron Velocity Selector, used in conjunction with the 45-MeV electron linear accelerator, produces pulses of essentially monoenergetic neutrons. Figure 1 shows the relative positioning of the electron-beam target, neutron-beam moderator, rotating mechanical beam chopper, scattering sample position, and neutron-beam detectors. Additional experimental details of the mechanical arrangement are reported elsewhere.[1-4]

*Dr. H. L. McMurry of NRTS, Idaho, has kindly provided some computations made for exact comparison with our data.

For the experiments reported here, the chopper spun at a speed of 180 rps. This operation provided a fundamental spread ΔE_o in incident energy E_o, essentially given by $2\tau/t \times E_o$, where τ is the effective full width at half maximum of the beam impinging on the scatterer, and t is the flight time required by neutrons with E_o to travel from the neutron-beam moderator to the chopper (~6.0 m). Table I gives a tabulation of the incident energies used in these experiments and the pertinent values of ΔE_o as a function of E_o. The measured energy resolution of the scattered neutrons, estimated below as $(\Delta E)_{calc}$, is poorer because of the shorter 2-m flight path from the scatterer to detectors. The computer program has been devised to take into account the effect on resolution of the flight paths, chopper-open time τ, and finite neutron-source emission time. A summary of typical results is also included in Table I, where the calculated spread $(\Delta E)_{calc}$ is given as a function of E_o and E. The energy transfer ϵ, which equals E_o-E, is also listed. The program can compute the effect of a spread (or natural width) in a level which gives rise to ϵ. For the results in Table I, however, this spread was assumed to be zero. The width $(\Delta E)_{calc}$ is thus due to instrumental broadening. An energy transfer ϵ due to an infinitely sharp level would always be broadened by ΔE_o, but the measured width would be still broader, as predicted by $(\Delta E)_{calc}$.

Two samples of polyethylene were used for these experiments. One, which was specially prepared for this research,* is a high-density (0.963 g/cc), oriented specimen. X-ray measurements (see Appendix I) performed in this laboratory according to the procedure outlined by Matthews et al.,[11] as well as the high density, indicate that more than 90 percent of the sample consists of long chain molecules. The manufacturer expects the molecular weight to be 70,000 to 90,000; thus this specimen is approximately represented as $(CH_2)_{6000}$. The other specimens used were of a much lower degree of regularity. In fact, x-ray measurements indicated that for these cases, about 40 percent of the CH_2 radicals was in the amorphous state, consistent with the lower density of 0.920 g/cc. The thickness of the highly crystalline specimen was 0.013 in. for most of the measurements. Additional measurements were made, using a thickness of 0.029 in., to check on the effect of multiple scattering. The thickness of low-crystallinity specimens was about 0.011 in.

The technique for calculating the absolute scattering cross section (together with necessary corrections) has been previously described.[4] No specific corrections for multiple scatterings are included here. However, to minimize multiple scattering corrections, thin samples were

*Specially prepared, by courtesy of Messrs. J. V. Cavender and R. E. Cairns, at Monsanto Company, Texas City, Texas.

used. The transmission of the specimens used in most of the measurements is large, of the order 0.90. The thickness of the vanadium scatterer standard was 0.079 in. All scattering specimens were placed at 45 deg to the incident neutron beam.

3.2 Experimental Results

The Neutron Velocity Selector has been used to study the detailed neutron scattering by "thin" layers of polyethylene. Precision cross-section measurements have been made with incident neutron energies of 0.167, 0.233, 0.408, and 0.499 eV, using a highly crystalline specimen. Additional measurements have also been made on less crystalline specimens having amorphous components forming approximately 40 percent. Typical of these latter specimens are the time-of-flight distributions shown in Figure 5. These two outwardly identical specimens give very different scattering results, one showing essentially no evidence for energy-level structure and the other showing rather pronounced level structure. The pattern with detailed structure gives the scattering cross section shown in Figure 6. As will be shown later, the structure in this scattering cross section is more pronounced than that observed for the crystalline scattering specimen, and the locations of some of the levels are somewhat shifted. This indicates a different internal structure of the molecules. For this reason, the amorphous specimens are not used in the detailed comparisons with theory.

Using the highly crystalline specimen of polyethylene, we have determined the scattering patterns for deflection angles of 30 deg, 60 deg, 90 deg, and 150 deg. A useful procedure is to derive the angular cross section $d\sigma/d\Omega$, which can be used to compare with independent, experimental data measured by Kirouac et al.[12] and, by integration, with the total scattering cross section data recently measured by Armstrong.* Figure 7 illustrates the angular dependence of the scattering per CH_2 radical for neutrons with 0.408 eV incident energy. Integrating this distribution according to

$$\sigma_{sc} = \int_0^{\pi} (d\sigma_{sc}/d\Omega \, 2\pi \, \mathrm{Sin}\,\theta d\theta$$

gives σ_{sc} = 50 barns, in good agreement with Armstrong.* Table III illustrates the acceptable nature of the agreement between these data and those of Kirouac et al.[12] and Armstrong*. It will be noted that the data of Kirouac et al., were obtained not at 30 deg but at 25 deg where their cross section should be somewhat larger. Their scattering specimen

*S. Armstrong, private data from Rensselaer Polytechnic Institute

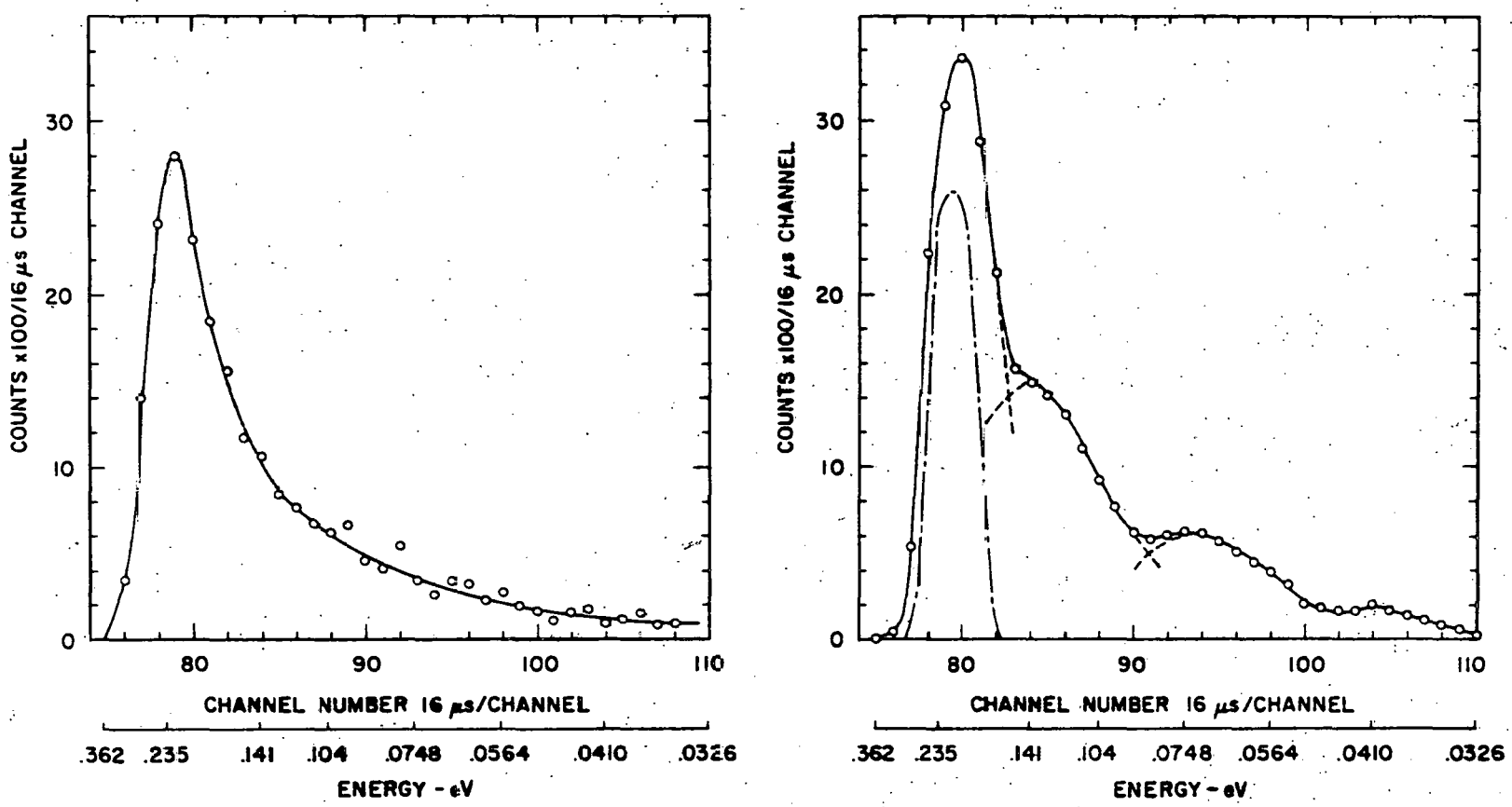

Fig. 5--Scattering patterns for two specimens of amorphous polyethylene, obtained at 90 deg with neutrons having incident energy of 0.235 eV

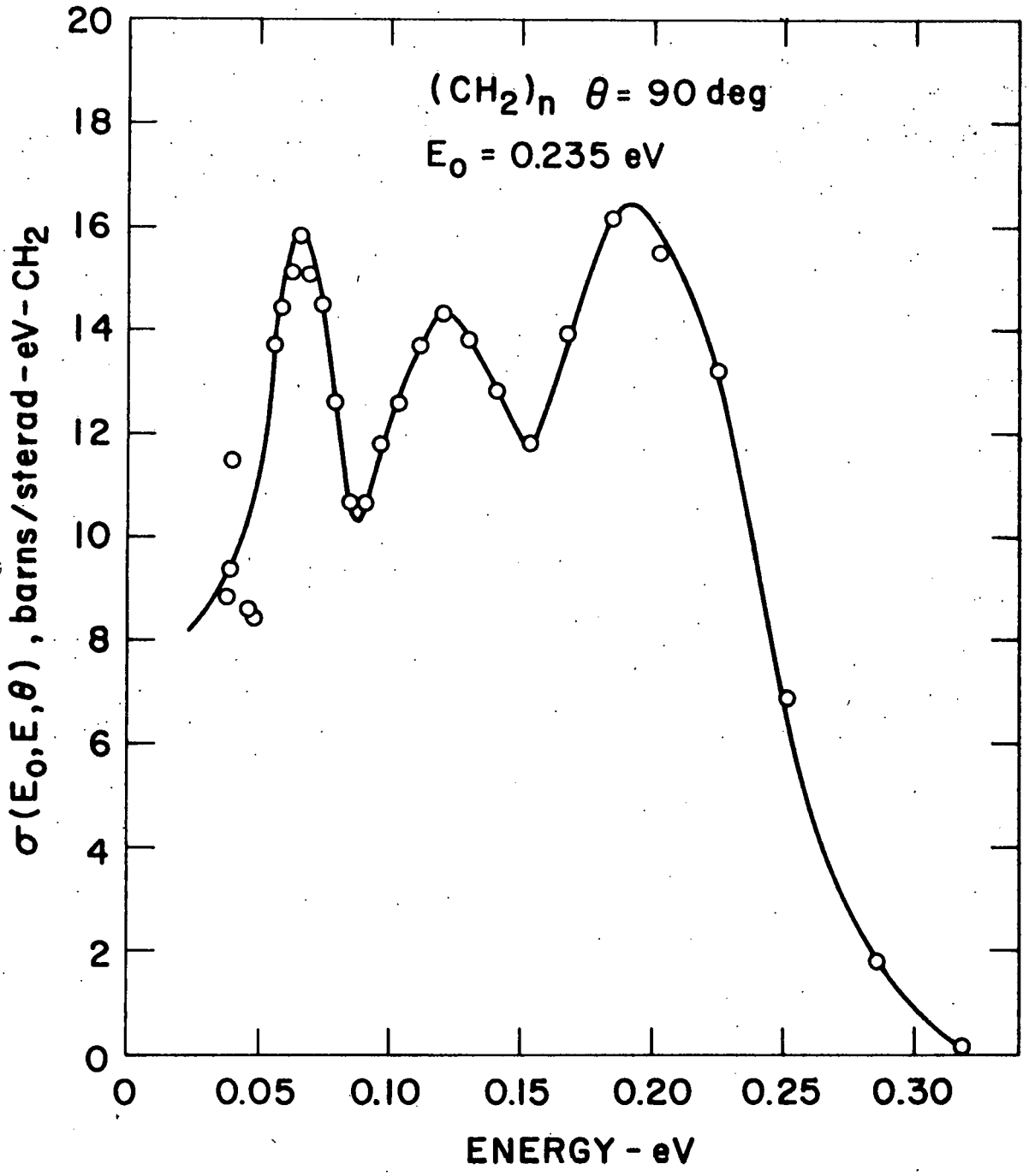

Fig. 6--Differential scattering cross section of specimen of amorphous polyethylene observed at 90 deg with neutrons of incident energy 0.235 eV

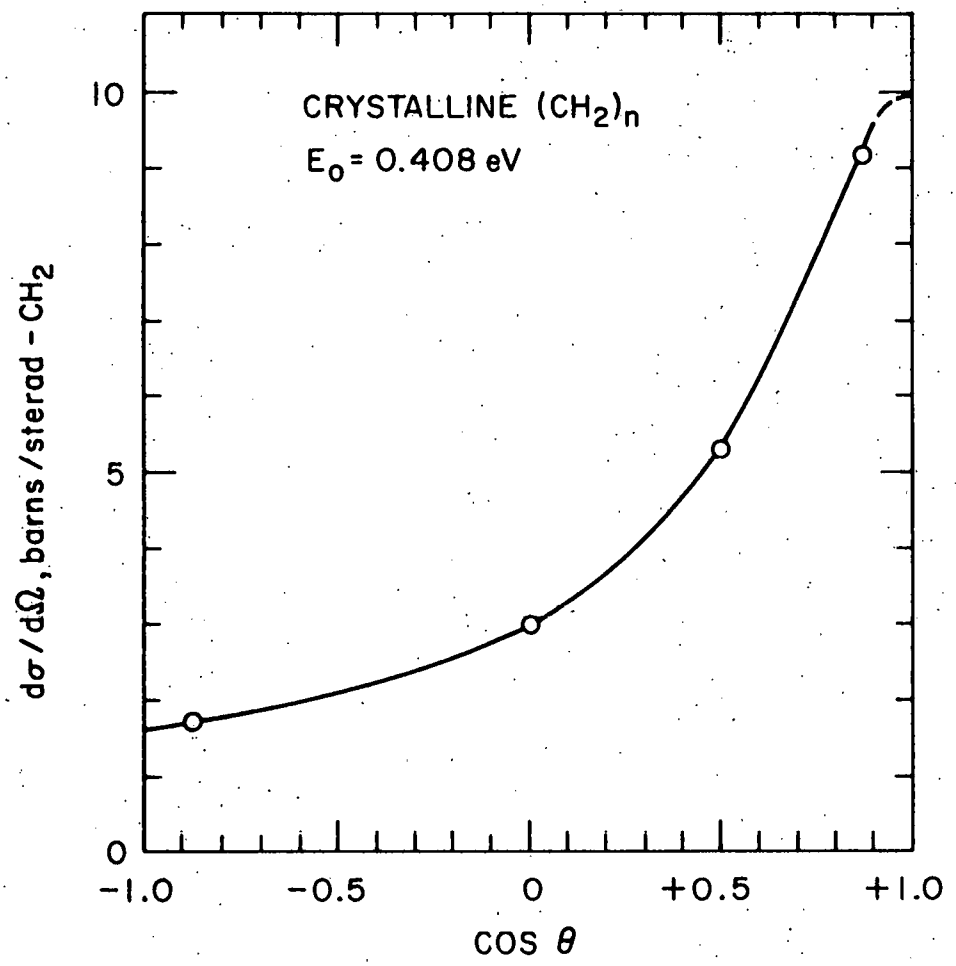

Fig. 7--Angular distribution of neutrons scattered by thin (0.013 in.) crystalline specimen of polyethylene

(0.020 in.) was somewhat thicker than that used for the present experiment (0.013 in.). It would appear, further, that their data at 0.233 eV are systematically too great, since the present, smaller values already integrate to a slightly too large total cross section.

TABLE III

A Comparison of the Experimental Angular and Total Scattering Cross Section with the Data of Armstrong and Kirouac et al.

E_o (eV)	$d\sigma_{sc}/d\Omega$, barns/sterad-CH_2				σ_{sc}, barns/CH_2	
	30 deg	60 deg	90 deg	150 deg	Integrated Values of $\sigma(E_o, E, \theta)$	Determined from Transmission Data[a]
0.167	10.6	5.8	3.4	2.0	57	62
0.233	10.3 (11.0)[b]	5.8 (6.3)	3.6 (3.8)	-- --	57.8	56
0.408	9.2 (10.5)	5.3 (5.4)	3.0 (2.8)	1.7	50	50
0.499	9.3 (9.6)	--	--		--	50

[a] S. Armstrong, private data from Rensselaer Polytechnic Institute.

[b] Data shown in parenthesis is that of Kirouac et al. (Ref.12) and was taken at 25 deg rather than 30 deg.

Before considering in detail the scattering data from crystalline polyethylene, it may be useful to observe experimentally the effect of using a scattering specimen of greater thickness. Figure 8 illustrates this effect for neutrons of 0.167 eV scattered at 30 and 90 deg and 0.408 eV at 90 deg. It will be seen that the effect of thickness over the transmission range used here (0.90 and 0.80) is small for the quasi-elastic scattering ($E_o \simeq E$), but is more pronounced for larger energy transfers. Experimental results for final energy below about 0.025 eV tend to be unreliable because of background effects. Based on extensive comparisons made at several incident energies and scattering angles, one can summarize

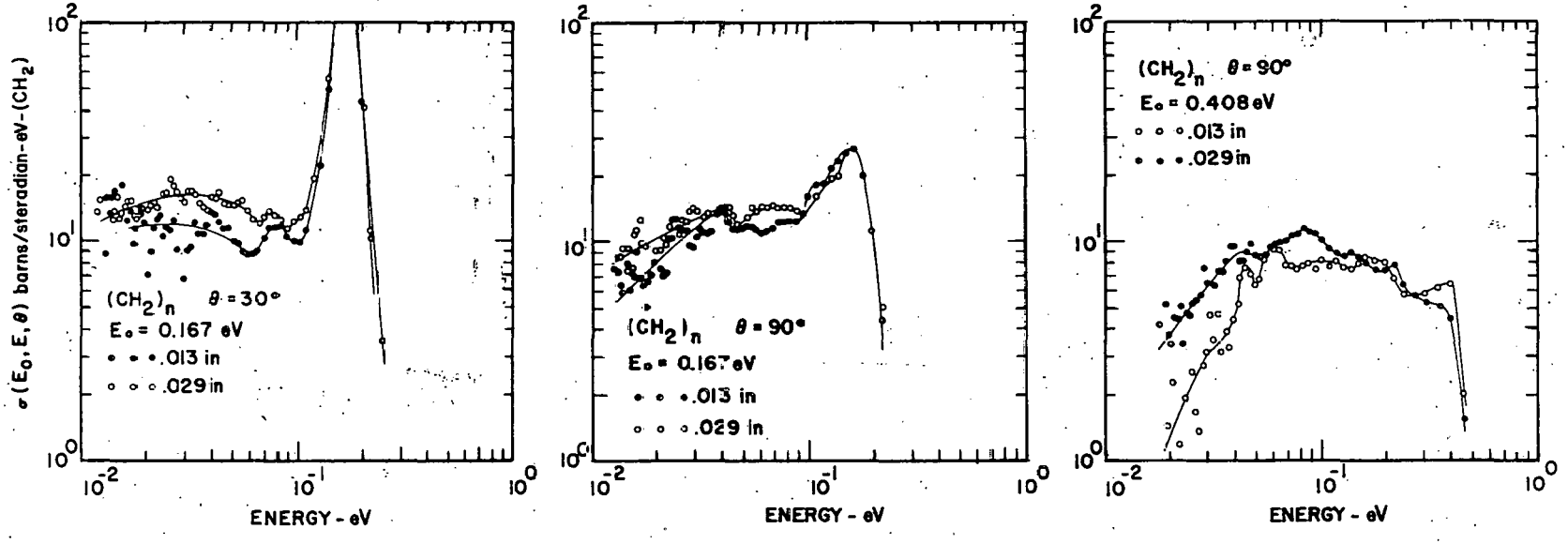

Fig. 8--A comparison for multiple scattering purposes of the scattering in $(CH_2)_n$ having thicknesses of 0.013 in. and 0.029 in., with varying E_o and θ

the experimental results made with the two thicknesses by noting that: a) the thicker scatterer tends to smooth some of the structure evident in the results with thinner specimens, and b) the thicker scatterer gives better statistical accuracy for the large energy transfers where there tend to be very few counts. Because of the increased effect of multiple scattering as a result of the increased scattering cross section of bound hydrogen at low final energies, the apparent statistical accuracy may not be significant. One concludes that the effect of multiple scattering is probably not larger than 10 to 15 percent for most energy transfers, but may become significantly larger for thicker scatterers ($T \geq 0.8$) and for energy transfers with very small final neutron energy ($\lesssim 0.025$ eV).

Typical experimental scattering data for neutrons with incident energies centered around 0.167, 0.233, 0.408, and 0.499 eV are exhibited in Figures 9-12. All of the data were obtained with the "thin" (0.013 in.) crystalline specimen of polyethylene. Typical statistical errors are indicated in each graph. Some theoretical results of McMurry are also shown in these figures. These will be discussed below. Also shown in the figures are some typical scattering results of Kirouac et al.,[12] which are consistent with the present results. The experimental techniques used to obtain these two sets of data are essentially the same except that Kirouac et al.,[12] used a thicker scattering specimen and may therefore have experienced in some degree the multiple scattering effect discussed above.

It may be interesting to compare the scattering data of Figures 6 and 10 for similar incident neutron energy scattering angle. It will be seen that the data obtained with the amorphous specimen (Fig. 6) give more pronounced energy levels and, in particular, the level corresponding to transfers of ~0.1 eV is far more prominent than in Figure 10 for the crystalline specimen. Presumably, this amorphous specimen has somewhat altered modes of motion due to its large collection of shorter molecules. For this reason, the data obtained with this specimen are not used in the comparisons with theory, since the theorists usually consider very long, single chains of CH_2.

The reader may be interested in the shape of the essentially elastic scattering distribution. As mentioned above, the resolution of the apparatus is such that a very narrow elastic peak appears broadened. For the experimental arrangement used, the incident energy ranges around E_o by an amount ΔE_o already evaluated in Table I. Typically, the widths of the quasi-elastic peaks exhibited in Figures 9-12 appear to be about three times the widths in Table I because of the shorter pathlength between scatterer and detector. Normally, one must use this latter, larger broadening as resolution. However, for the case discussed below, which is typical of several similar cases, one may estimate rather well the effective, smaller width ΔE_o defined above. In order to check on the validity of doing this,

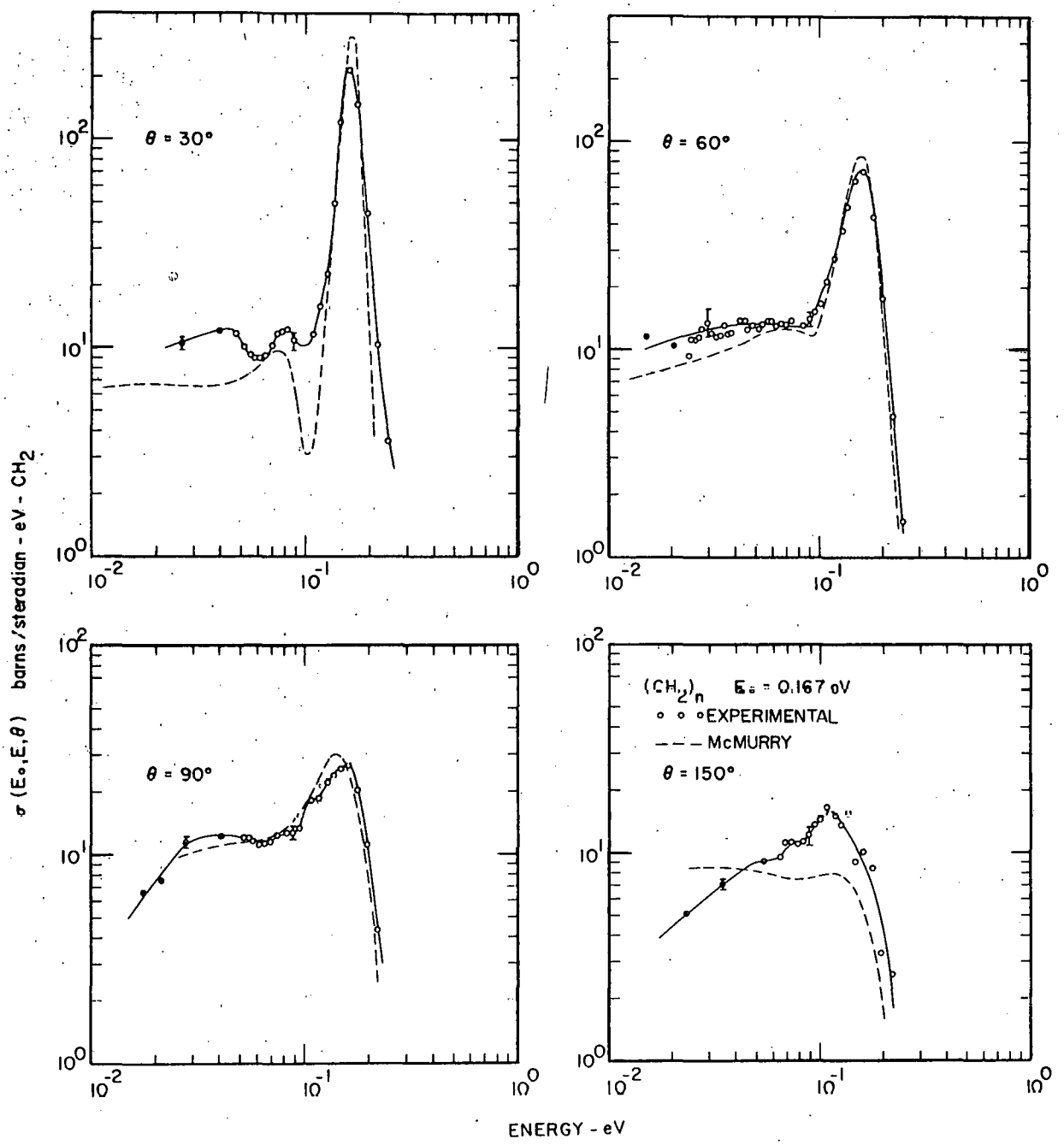

Fig. 9--Scattering of 0.167 eV neutrons by crystalline polyethylene

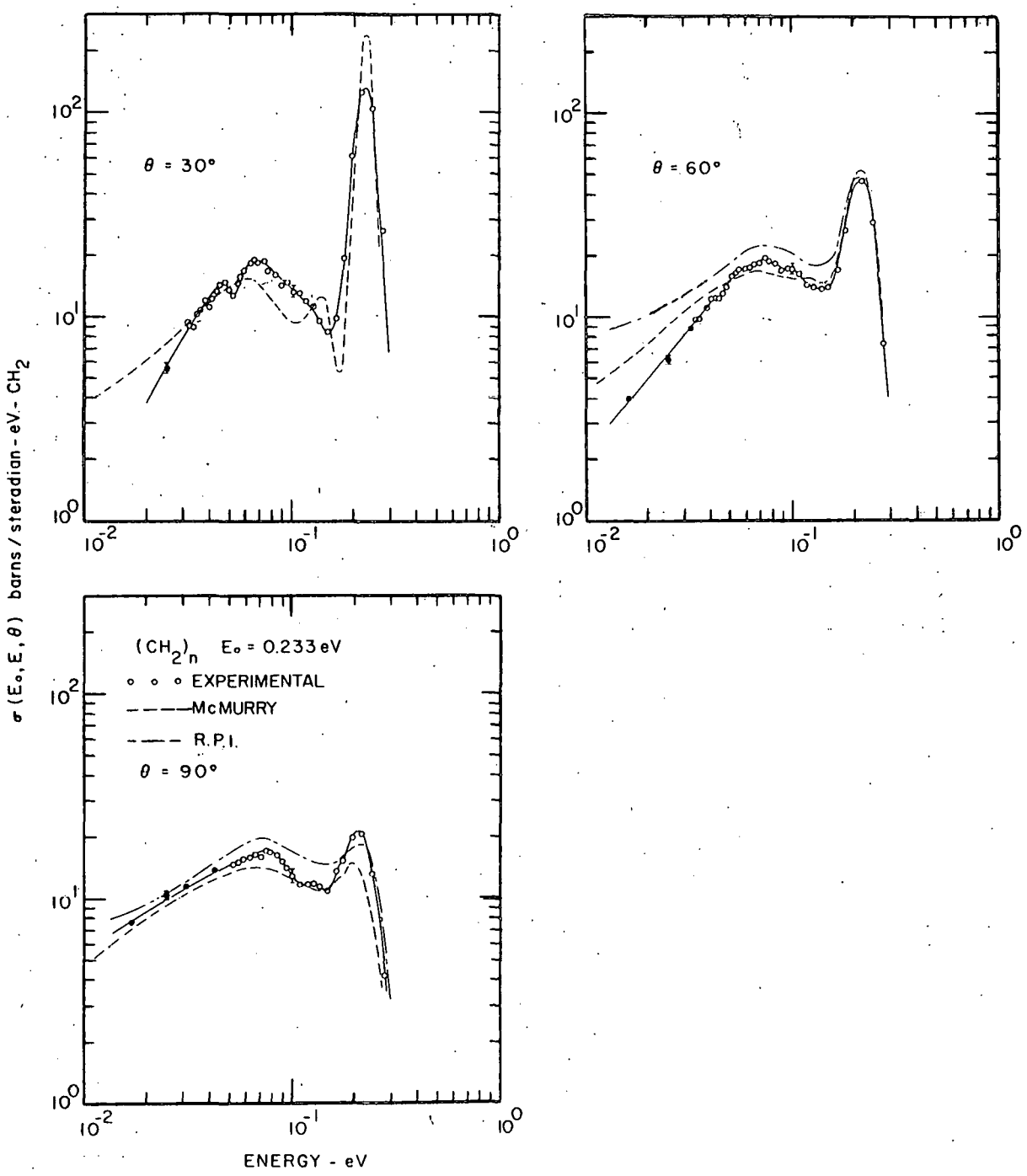

Fig. 10--Scattering of 0.233 eV neutrons by polyethylene

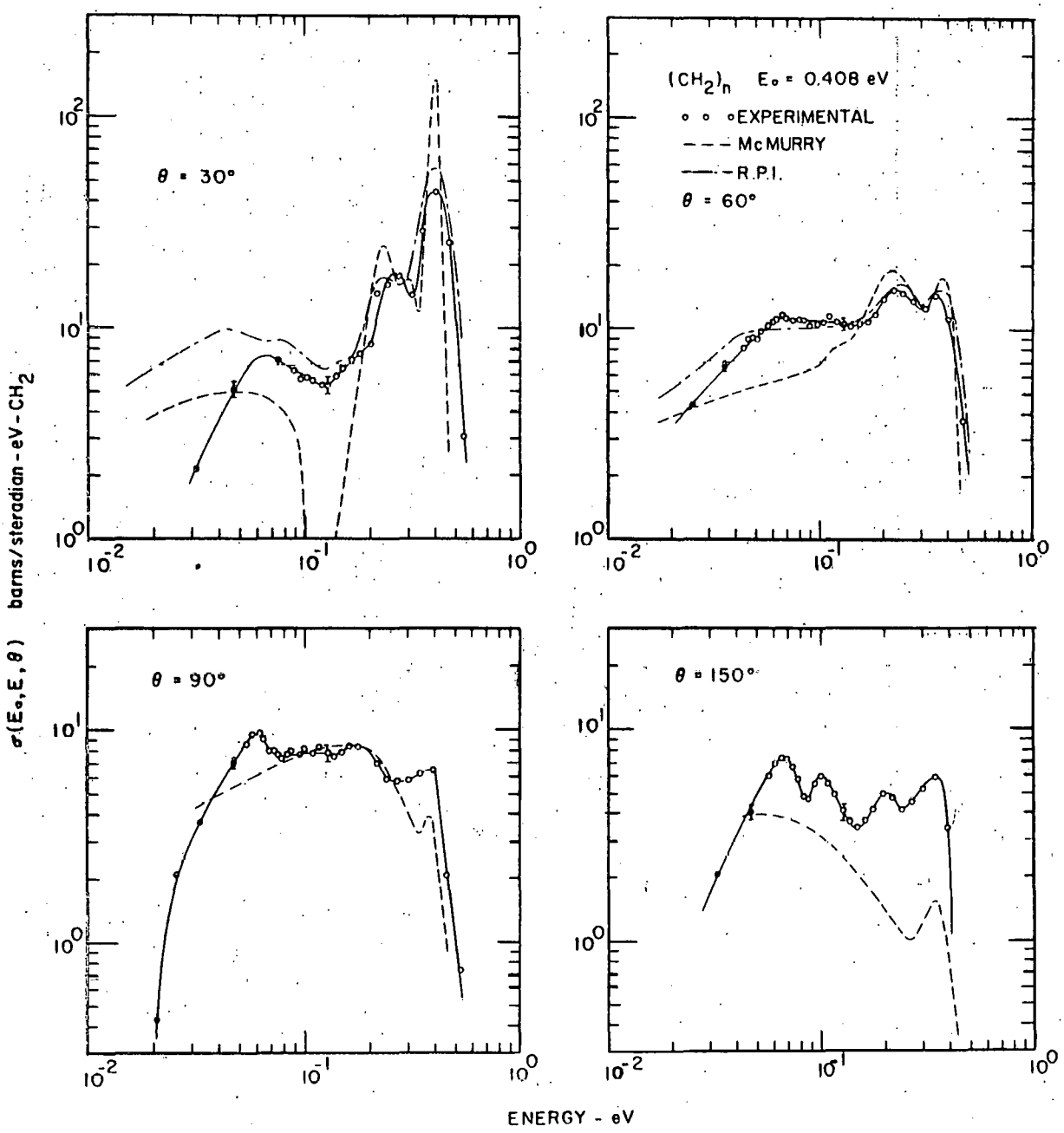

Fig. 11--Scattering of 0.408 eV neutrons by polyethylene

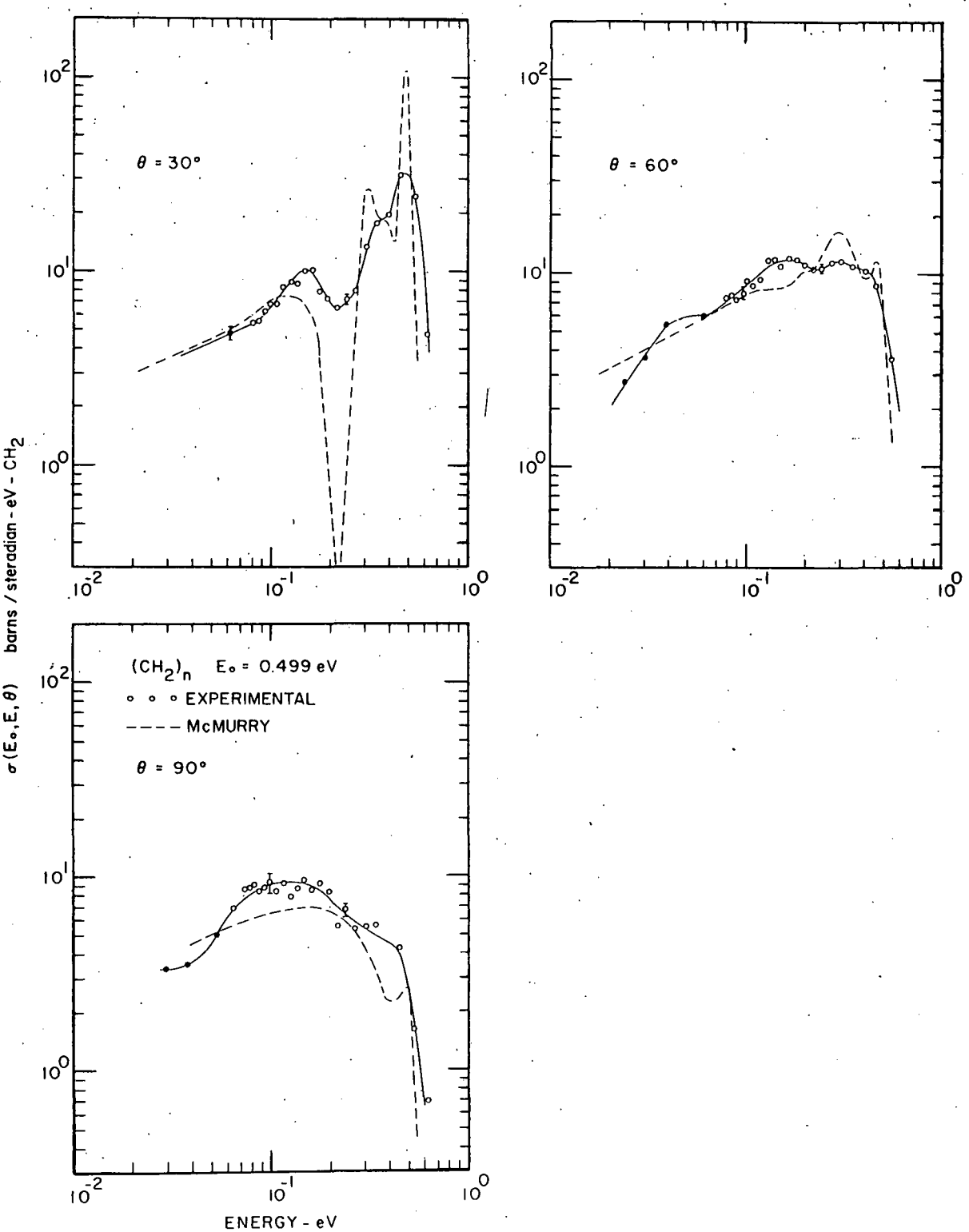

Fig. 12--Scattering of 0.499 eV neutrons by polyethylene

one has only to compare the elastic peaks for scattering by the sample and by a "thin" specimen of vanadium and be sure that these two distributions have essentially the same width. One can then deduce that the width of the elastic peak for the scattering cross section is at least as narrow as ΔE_o. Making a reasonable division between the inelastic and elastic scattering for $E_o \simeq E$, one can correct the shape of the scattering cross section, as has been done in Figure 11 for the results at E_o = 0.408 eV at 30 deg. This modification can be seen in greater detail in Figure 13. This technique can, of course, be successfully applied only when the elastic-scattering pattern of vanadium indicates that, effectively, only elastic scattering is involved.

3.3 Discussion of Results

As noted in the Introduction, several authors have attempted to derive an appropriate scattering cross section for polyethylene. In general, the treatment is either quite exact, where the utilization of a realistic frequency distribution is attempted (Parks[8]), or approximate, where the real frequency distribution is variously represented by three, four, or five discrete frequencies (Goldman and Federighi,[7] Koppel and Young,[10, 13]).

The trial frequency distribution derived by Parks to fit the acoustic and optical parts of the spectrum is illustrated in Figure 14. The frequency distribution $f(\omega)$ used by Parks[8] is derived from the distribution $\rho(\omega)$ obtained from infrared and specific heat data by Wunderlich[14]. The distribution $\rho(\omega)$ enters directly into the determination of the thermodynamic properties of polyethylene, but not into the determination of neutron scattering in the gaussian approximation. To obtain the latter, we require not only the distribution of frequencies, but also the distribution of amplitudes of vibration. Parks[8] makes the crude assumption that in the acoustical branch and in the c-c stretch mode of the vibration spectrum, the H and C atoms move in phase. Since the effective mass in these modes must be 14, that in the remaining optical modes must be 14/13.

If $\rho_{ac}(\omega)$, $\rho_{cc}(\omega)$ denote the densities of mode associated with the acoustical, the c-c stretch, and the optical modes, respecitvely, and if

$$\int [\rho_{ac}(\omega) + \rho_{cc}(\omega)]\, d\omega + \int \rho_{op}(\omega)\, d\omega = 1 \ , \qquad (3)$$

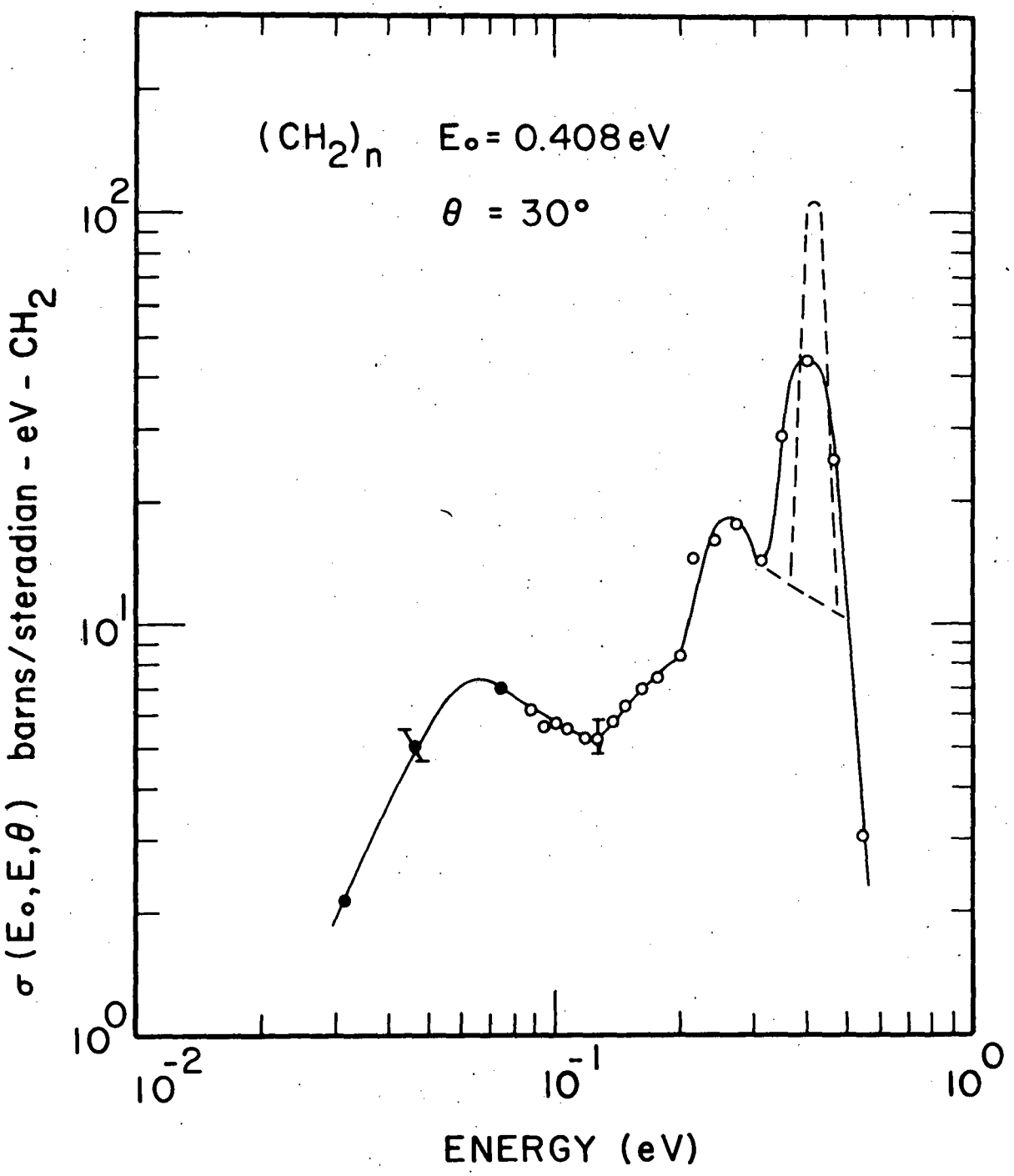

Fig. 13--Scattering of 0.408 eV neutrons at 30 deg by polyethylene. Note the estimated broadening of the elastic peak caused by instrumental resolution

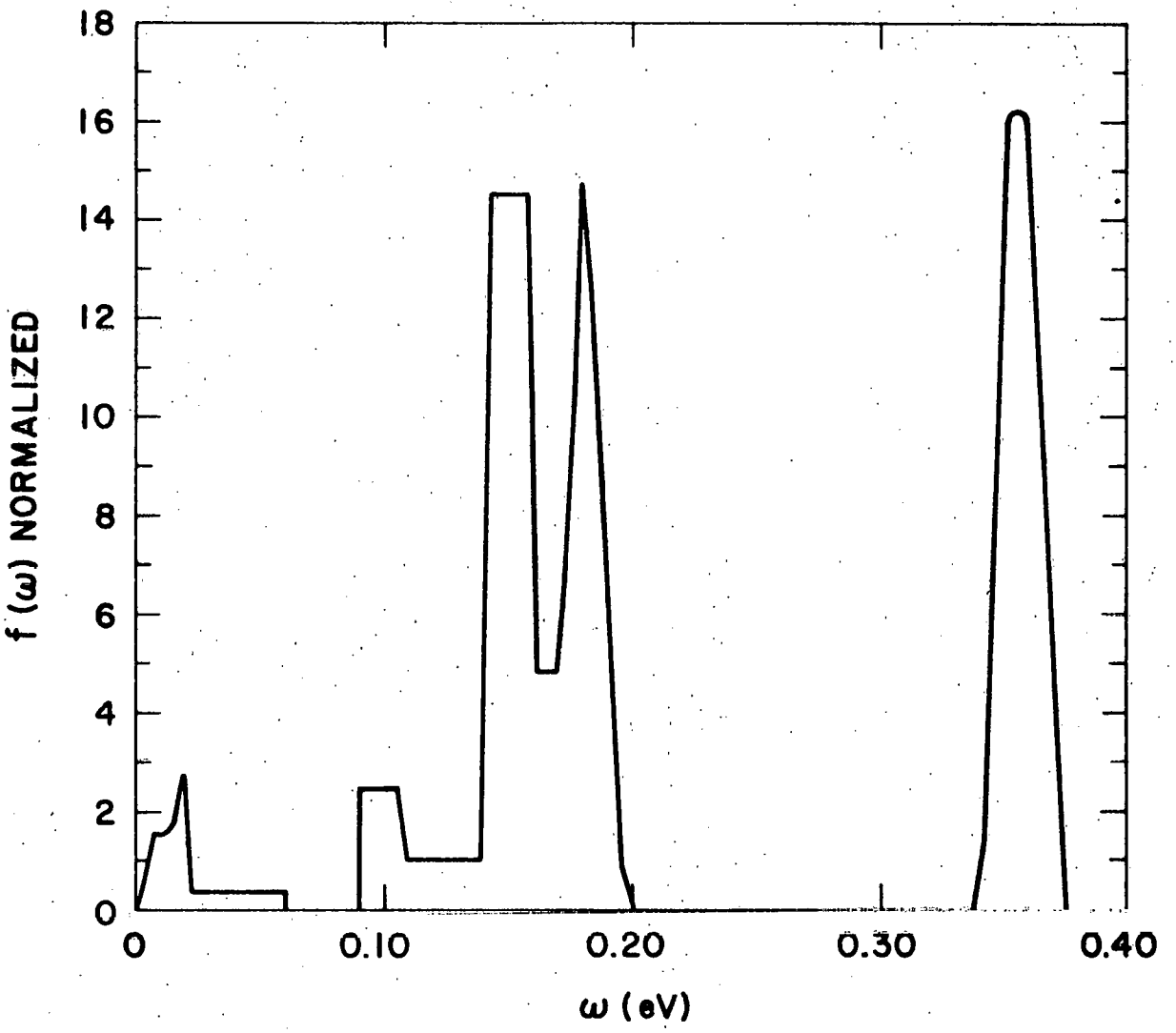

Fig. 14--Frequency distribution used by Parks for calculation of differential scattering cross section of polyethylene

then

$$f(\omega) = \frac{\alpha\,[\rho_{ac}(\omega) + \rho_{cc}(\omega)] + (1-\alpha)\,\rho_{op}(\omega)}{\alpha \int [\rho_{ac}(\omega) + \rho_{cc}(\omega)]\,d\omega + (1-\alpha) \int \rho_{op}\,d\omega} \quad , \tag{4}$$

where α is chosen so that

$$\frac{\alpha \int [\rho_{ac}(\omega) + \rho_{cc}(\omega)]\,d\omega}{\alpha \int [\rho_{ac}(\omega) + \rho_{cc}(\omega)]\,d\omega + (1-\alpha) \int \rho_{op}(\omega)\,d\omega} = \frac{1}{14} \quad . \tag{5}$$

Using the following relations taken from Reference 2,

$$\int \rho_{ac}(\omega)\,d\omega = 2 \int \rho_{cc}(\omega)\,d\omega = \frac{2}{9} \quad ,$$

$$\int \rho_{op}(\omega)\,d\omega = \frac{2}{3} \quad ,$$

we find that

$$\alpha = \frac{2}{15} \quad .$$

The differential scattering cross section is derived from the frequency spectrum of Figure 14 by use of the code SUMMIT, which sums over 15 phonon contributions to the scattering cross section. SUMMIT has given neutron spectra in good agreement with experiment.[8] It predicts acceptable total cross-section data in the energy range below ~0.3 to 0.4 eV, but underestimates the cross section in the higher energy range, probably as a result of the limited number of phonons used in the calculation. The cross sections derived by SUMMIT are compared with the current experimental differential data, in Figures 15 and 16.

The discrete oscillator treatment of the frequency spectrum, using the Nelkin procedure for water,[9] has been attempted first by Goldman and Federighi,[7] and later repeated by Koppel and Young[10] with a differently chosen set of discrete oscillators. In the comparisons to follow,

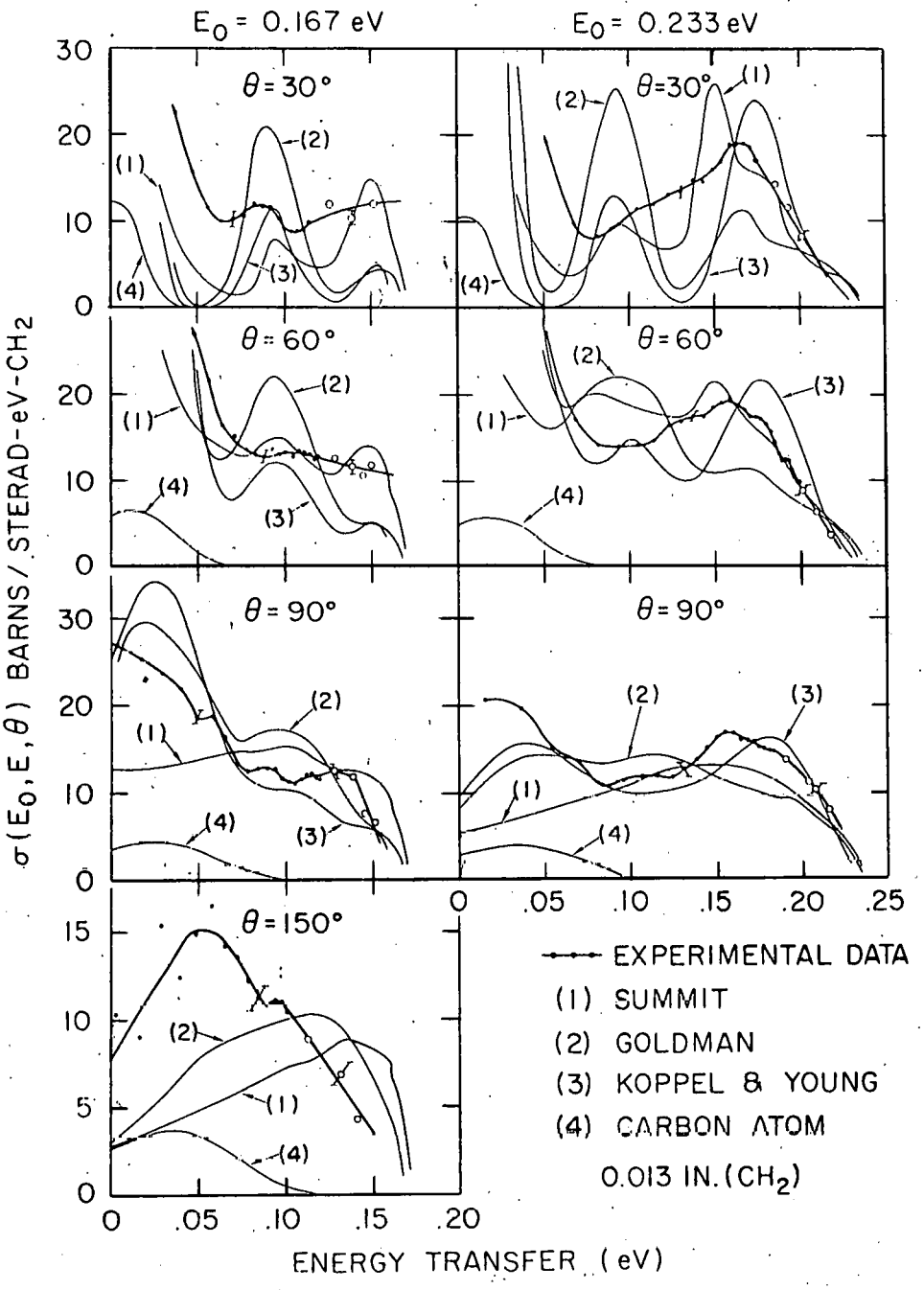

Fig. 15--Differential scattering cross section of polyethylene plotted as function of energy transfer for neutrons with incident energies of 0.167 and 0.233 eV. Theoretical treatments of Parks (1), Goldman (2), and Koppel and Young (3) are included for comparison. Scattering by carbon atoms is illustrated by curve (4)

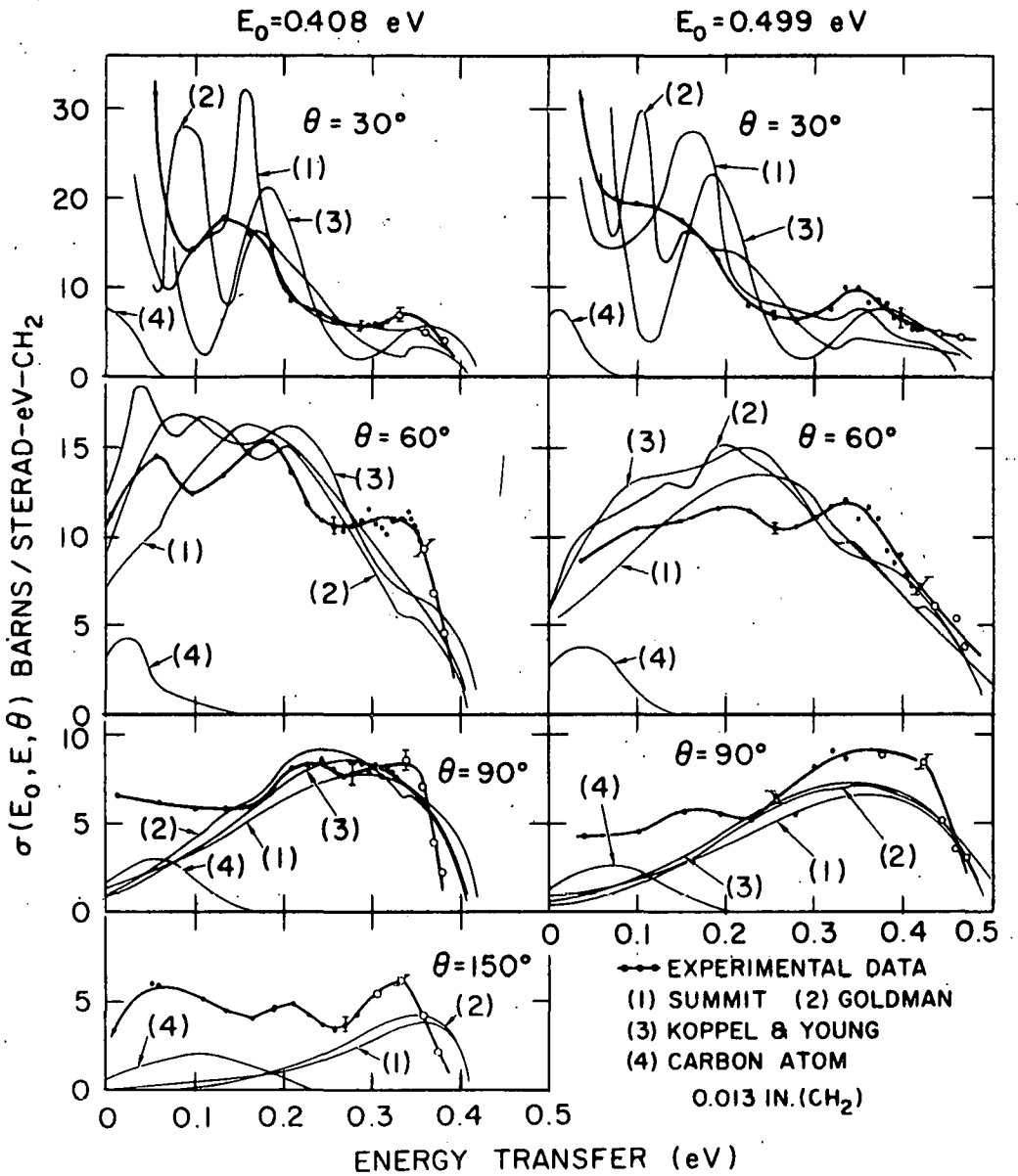

Fig. 16--Differential scattering cross section of polyethylene plotted as a function of energy transfer for neutrons with incident energies of 0.408 and 0.499 eV. The theoretical treatments of Parks (1) Goldman (2), and Koppel and Young (3) are included for comparison. The scattering by carbon atoms is illustrated by curve (4)

the Goldman cross section has been computed* for a portion of the experimental conditions, using oscillator levels at 0.089, 0.160, 0.187, 0.353, and 0.533 eV. The comparison with experimental data is made in Figures 15 and 16. A scattering cross section has been derived by Koppel and Young[13] using either three or four discrete oscillators. In both cases, they omit the 0.533-eV level, since the work of Lin and Koenig [15] indicates that the most energetic level in polyethylene occurs at ~0.36 eV. We have chosen, for comparison, Koppel and Young's cross section based on three frequencies, since this is the more radical departure from Goldman and Federighi's five-frequency spectrum.[7] Table IV indicates Koppel and Young's choice of oscillator frequencies and relative weights. Of course, it is recognized that the smaller number of oscillators will further exaggerate the apparent structure of the scattering cross section, but it eliminates some of the technical switching problem created by the use of GAKER code. A comparison of this cross section with the experimental data is made in Figures 15 and 16.

TABLE IV

Oscillator Frequencies of Koppel and Young[a] for Polyethylene (Spectrum B)

Oscillator Level (eV)	Normalized Weight
0.09	0.1005
0.170	0.4930
0.360	0.3350
0 (translation)	0.0715

[a]See Ref. 13

In the cross section generated by SUMMIT, purely elastic scattering ($E_o = E$) and scattering from the carbon in $(CH_2)_n$ have been omitted. Goldman, and Koppel and Young include the elastic scattering by including a zero-frequency translational component with mass 14, but omit the carbon atom scattering. For completeness, elastic scattering and carbon-atom scattering are evaluated here (see Parks et al.[16]). Purely elastic scattering from H atoms bound in polyethylene is given in Eq. (2-112) of

*The computed cross section data have been kindly supplied by D. T. Goldman, KAPL.

Reference 16 as

$$\frac{d^2\sigma_{el}(H)}{dEd\Omega} = \frac{\sigma_b}{4\pi} e^{-2W} \delta(E_o - E) \quad , \tag{6}$$

where

$$2W = \frac{\kappa^2}{2M} \int_{-\infty}^{+\infty} \frac{f(\omega)\, e^{\omega/2kT}}{2\omega \sinh \omega/2kT}$$

$$= \frac{\kappa^2}{2} \times 8.68886, \text{ and}$$

$$\frac{\kappa^2}{2} = E_o + E - 2\sqrt{E_o E} \cos\theta ,$$

σ_b = 81.44 barns,

δ = Dirac delta function.

Of course, this scattered beam will be spread out by the instrumental resolution in a real experiment. The scattering by carbon atoms is crudely given as

$$\frac{d^2\sigma}{dEd\Omega} = \frac{4.8}{4\pi} \left(\frac{1}{1-\alpha}\right) \frac{1}{E_o} \quad , \tag{7}$$

where $\alpha = (A - 1/A + 1)^2 = 0.715$,

A = atomic weight of scattering atom, and

$\alpha E_o \leq E_o$.

A better representation of this scattering is given by the free gas approximation:

$$\frac{d^2\sigma}{dEd\Omega} = \frac{\sigma_o \left(\frac{M+1}{M}\right)^2}{4\pi} \sqrt{\frac{E}{E_o}} \left(\frac{M}{2\pi \kappa^2 kT}\right)^{\frac{1}{2}} \exp\left[\frac{\left(-M\ E_o - E - \frac{\kappa^2}{2M}\right)^2}{2\kappa^2 kT}\right], \quad (8)$$

where σ_o = 4.8 barns,

M = 12,

kT = thermal temperature of scatterer, and

$\frac{\kappa^2}{2}$ is as defined above.

Typical values of the hydrogen-atom elastic scattering are given in Table V. It is observed that the purely elastic contribution is small compared with the observed quasi-elastic scattering for the same energy, as shown in Figures 9-12. This computed contribution will be greater for small incident energy, where the momentum transfer is also small. The carbon contribution has also been computed and, in Figures 15 and 16, is compared directly with the experimental results. The contribution due to carbon scattering is a significant correction to the theoretical curves, particularly at the larger angles.

TABLE V

Computed Elastic Scattering Cross Section of Hydrogen

E_o	$d^2\sigma_{el}/dEd\Omega$, barns/sterad-eV-H atom				
(eV)	30	60	90	120	150
0.167	4.27	1.45	0.33	0.08	0.03
0.233	3.71	0.86	0.12	0.016	~0
0.408	2.45	0.18	~0	~0	~0
0.499	2.04	0.09	0.001	~0	~0

By reference to Figures 15 and 16, one observes that the theoretical treatments specified above give results which differ in their details, as expected. The SUMMIT treatment gives a generally smoother scattering cross section, with some evidence for the occurrence at low incident energies and small scattering angles of the structure observed in the frequency distribution shown in Figure 14. For larger scattering angles, particularly for large incident energies, the SUMMIT cross section is somewhat smoother than observed experimentally. For low incident energies (0.167 eV and 0.233 eV), SUMMIT predicts somewhat sharper features than observed and overemphasizes the importance of the band of oscillator levels near 0.09 eV. It shares this latter feature in common with, but to a lesser extent than, the discrete oscillator treatments of Goldman and Federighi and of Koppel and Young, as will appear below. For the larger incident energies (0.408 eV and 0.499 eV), the SUMMIT cross section overemphasizes the importance of the levels, particularly those near 0.18 eV, but underestimates the 0.36-eV level. The importance of elastic scattering from the carbon and hydrogen atoms has been mentioned above and, when added to this cross section, will serve to bring the SUMMIT prediction into fair agreement with the experimental data for small energy transfers around E_o. In summarizing the comparison with experiment, it appears that Parks' frequency distribution[8] should be altered to lessen the importance of the lower lying levels and to give greater weight to the highest energy transfers around 0.36 eV, due to the H-C motion.

The theoretical treatments of Goldman and Federighi and of Koppel and Young, when compared with the experimental results in Figures 15 and 16, tend to exhibit more structure than is observed experimentally at small scattering angles for all incident neutron energies. In particular, Goldman and Federighi predict results for the level 0.089 eV which are much too great in all cases. The data of Koppel and Young are similar in that they predict too much weight for the 0.089-eV level. For the low incident energies and larger scattering angles, both of these treatments agree reasonably well with the experiments. Similar conclusions are reached for the higher incident neutron energies ($\geq$ 0.4 eV). For all energies studied, better agreement between these theories and experiment is achieved if the carbon contribution is included.

Lest the reader attribute the lack of evidence for sharp levels in the experimental data to poor experimental resolution, we note that with similar incident energies, the sharp bound hydrogen levels in zirconium hydride ($h\nu$ = 0.14 eV), yttrium hydride ($h\nu$ = 0.12 eV), and lanthanum hydride ($h\nu$ = 0.103 eV) have been clearly observed.[1-4,17] Although the intermediate range of frequencies for polyethylene (0.089 - 0.18 eV) may be distributed, as deduced from the scattering data, one expects that the energetic vibrational modes ($\sim$ 0.36 eV) should be rather sharp. Examination

of the experimental data for small scattering angles of 0.499 eV neutrons reveals a peak in the energy transfer at 0.35 eV, superimposed upon what appears to be the scattering due to multiphonon interactions. The peak has a full width of ~ 0.12 eV and half-width of ~ 0.06 eV. Reference to Table I shows that an infinitely sharp level at 0.36 eV would appear to have a width of at least 0.07 eV, consistent with the observed half-width. One thus concludes that the highest energy levels in polyethylene are indeed quite sharp.

The theoretical treatment of McMurry* has been separated from the other because his treatment was not specifically for polyethylene. As noted in the introduction to this section, McMurry computed results for n-butane, which contains limited numbers of methyl (CH_3) and ethyl (CH_2) radicals. He has computed separately and exactly the contribution to the scattering made by each of these radicals. In n-butane and polyethylene, one expects similar stretching and deformation modes. The sketetal modes associated with translational and rotational motions of the CH_3 and CH_2 radicals are also expected to be analogous to some of those in the polyethylene chain. Of course, the exact location of the appropriate bands of frequencies will be different than that for polyethylene. However, it may be interesting to observe how well these predictions for the CH_2 radical fit the experimental data.

An exact calculation of the ethyl radical (CH_2) contribution to the scattering was made and, in Figures 9-12, is compared with the experimental results. Data for E_o = 0.167 eV are shown in Figure 9. The sharpness of the theoretical details is somewhat too pronounced at 30 deg compared with the experiment, although the peak at energy transfers of -0.087 eV is in fair agreement. At 60 and 90 deg, the agreement is reasonably good. At 150 deg, however, the agreement is rather poor. In Figure 10, the results are shown for 0.233 eV scattering. The theoretical results at 30 deg show too much structure. The fit for θ = 60 and 90 deg is quite good. Figure 11 gives results for E_o = 0.408 eV. In this case, the theory predicts too little cross section for energy transfers of ~0.35 eV, as shown by the results for 60, 90 and 150 deg. The theoretical results predict too little "elastic" scattering for E_o = 0.408 eV at 90 and 150 deg. Figure 12 gives results for E_o = 0.499 eV. In this case, the theory predicts too much "elastic" scattering and, as before, too much structure at 30 deg.

In summarizing McMurry's theoretical efforts, it is well to recall that these results have been derived for n-butane. We are fortunate that it has been possible to extract results for the CH_2 radical from his C_4H_{10}

*See footnote, p. 17.

results. Since his normal mode calculations are for a molecule which is rather short compared with $(CH_2)_{6000}$, It is surprising that the results for the CH_2 radical fit the experiment as well as observed. It is expected that a normal mode calculation for $(CH_2)_n$ will improve the agreement still further and will yield results which are quite adequate for calculations of reactor parameters.

3.4 Scattering-Law Considerations

The comparison of the theoretical cross sections and experimental data can be made with sufficient accuracy to point out limitations or sufficiency of the theoretical model, using the scattering cross section only. This is illustrated above for the data available. To derive the Scattering Law, considerably more data are needed to provide any worthwhile, additional comparisons or deduce the frequency distribution. Using the data available, we will attempt to derive a frequency distribution, although in previous sections we have already stated the status of the theoretical cross sections available.

The Scattering Law $S(\alpha, \beta)$ used here has the usual definition[18] but will be repeated for completeness.

$$\frac{d^2\sigma}{dEd\Omega} = \frac{\sigma_b}{4\pi kT}\sqrt{\frac{E}{E_o}}\,[\exp(-\beta/2)]S(\alpha,\beta) \quad , \tag{9}$$

where $\alpha = (E_o + E - 2\sqrt{EE_o}\cos\theta)/Mkt$

$\beta = (E - E_o)/Mkt$

kT = thermal energy of specimen, and

M = 1, for mass of hydrogen scatterer in units of neutron mass.

The value of $S(\alpha, \beta)$ is that it is simply related to the various phonon contributions to the scattering. Specifically,

$$\frac{S(\alpha,\beta)}{\alpha} = a + b\alpha + c\alpha^2 + \ldots \tag{10}$$

where a, b, c, ... depend on β but not on α. Furthermore, a is determined completely by the one phonon term, b by the one and two phonon

term, etc. Egelstaff[18] has already pointed out that generalized frequency distributions $p(\beta)$ and $f(\beta)$ can be derived from $S(\alpha,\beta)/\alpha$. In his notation, we have

$$p(\beta) = \beta^2 \left[\lim_{\alpha \to 0} S(\alpha,\beta)/\alpha \right] \tag{11}$$

$$= \beta^2 a \text{; from Eq. (10)}$$

and

$$f(\beta) = \frac{\sinh(\beta/2)\, p(\beta)}{\beta/2} \tag{12}$$

The use of Eq. (11) to determine $p(\beta)$, and hence $f(\beta)$, is confused by the quadratic and higher order terms in Eq. (10), unless the extrapolation is performed for very small values of α. For the experimental cases at hand, it can be shown that the extrapolation is possible without significant contribution from the phonon terms above the first, if $\underline{\alpha} \ll 4$. This is impossible for the existing data obtained for the large incident energies unless very small angle scattering is studied ($\theta \ll 30$ deg). Since larger angles were used, significant effects of the higher order terms will be present in $p(\beta)$.

Figure 17 illustrates typical Scattering Law data for $0 < \beta < -6$. Additional, similar data exists for β ranging up to -16. When these data are plotted on semilog paper, as in the example shown in Figure 18, one observes reasonably linear curves over an extended range of $\underline{\alpha}$, although the values of $\underline{\alpha}$ are not small compared with $\underline{4}$, as required by the discussions above. Since the limited data give reasonably linear extrapolations, this procedure was followed for the available data, and the $p(\beta)$ curve shown in Figure 19 results. The accuracy of the data for transfers in the neighborhood of 0.35 eV is extremely poor because 1) the number of points on the $S(\alpha,\beta)/\alpha$ versus $\underline{\alpha}$, curve is very small, and 2) the extrapolation is made for large values of $\underline{\alpha}$, where higher-order phonon terms may predominate. The values of the extrapolation for these large energy transfers should be statistically accurate, since most of these data come from curves like those shown in Figure 12 for 0.499 eV neutrons, where a rather well-determined bump in the scattering cross section is observed for energy transfers of ~0.35 eV. Using the relation between $f(\beta)$ and $p(\beta)$ in Eq. (12) and the experimental values of $p(\beta)$, one can derive a frequency distribution for polyethylene, shown in Figure 20. An estimate of the accuracy of the extrapolation results is also included as well as typical energy resolutions. It must be remembered that this curve is probably distorted because of a large contribution from the higher-order phonon terms. Also shown in Figure 20 is the theoretical frequency distribution of Parks, used in the

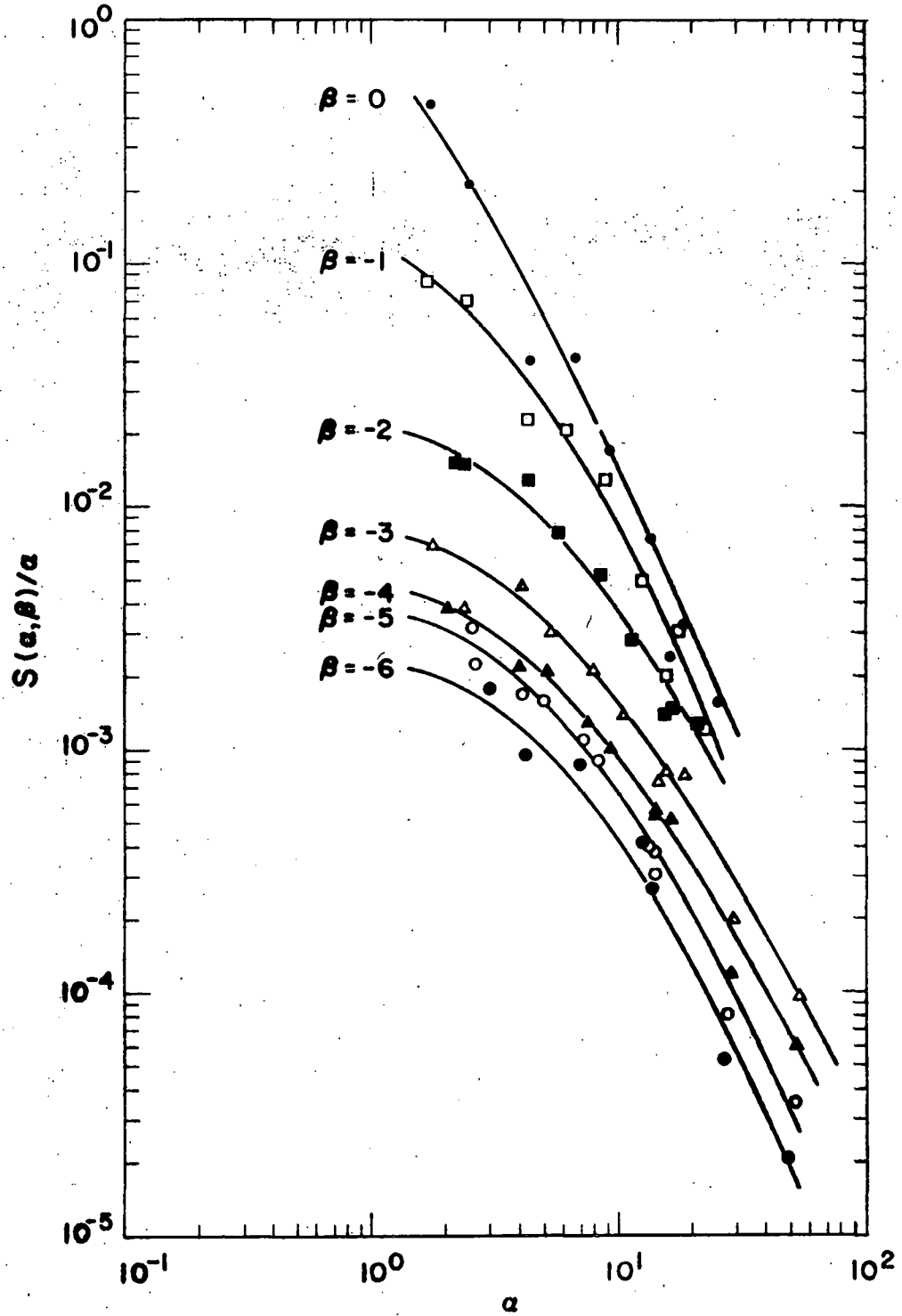

Fig. 17--Typical Scattering Law data for crystalline polyethylene obtained with incident neutron energies in the range 0.167 to 0.499 eV

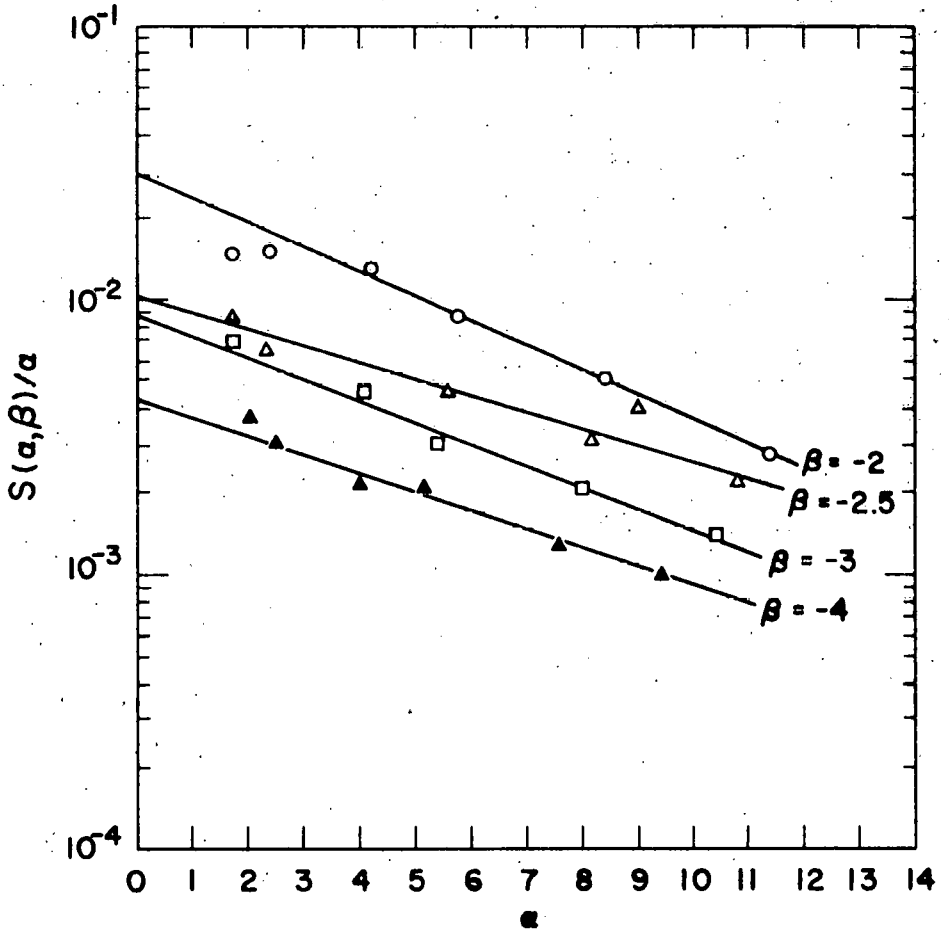

Fig. 18--Typical Scattering Law data used to extrapolate $S(\alpha,\beta)/\alpha$ to $\alpha = 0$

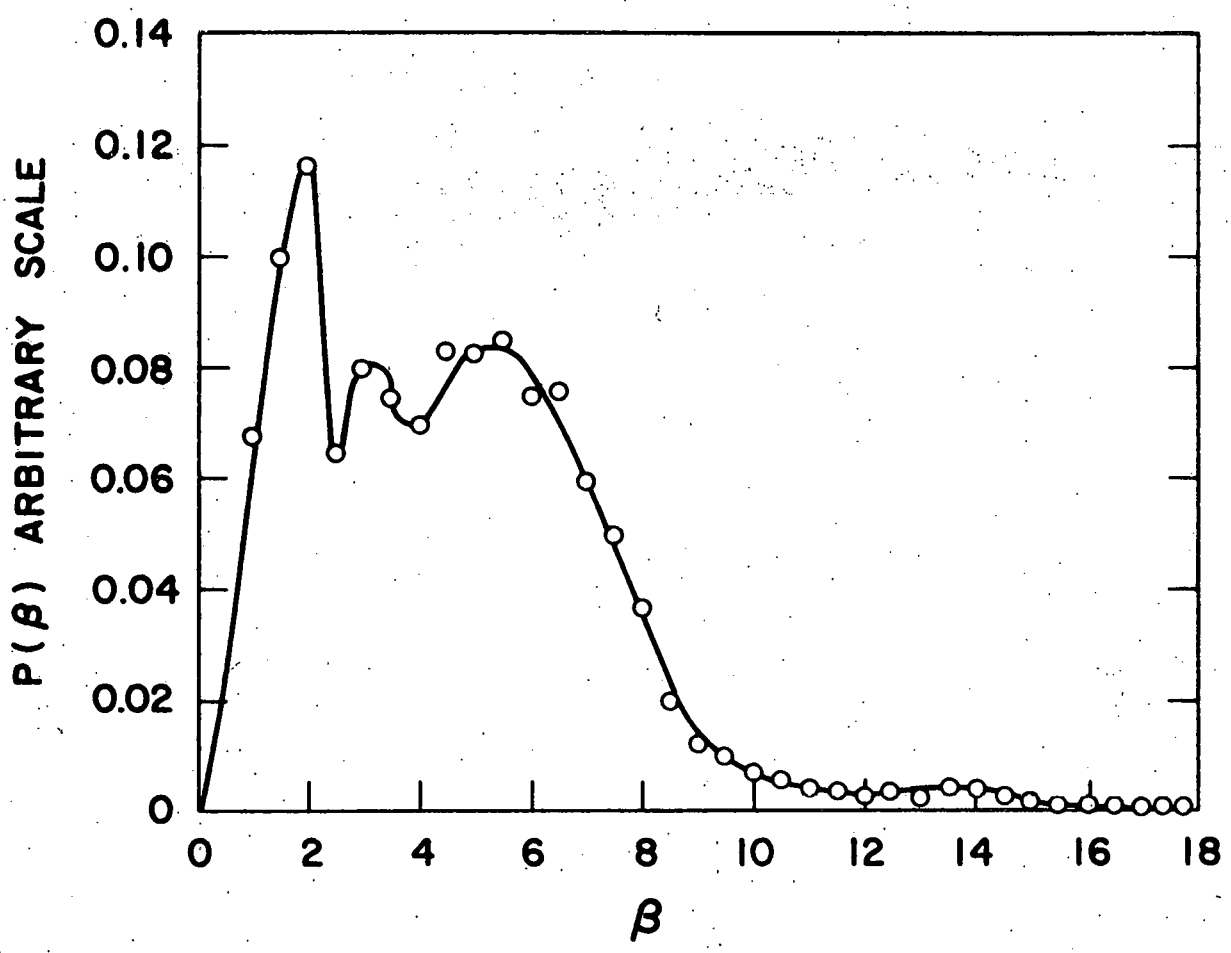

Fig. 19--The generalized frequency distribution p(β) derived using the extrapolation technique

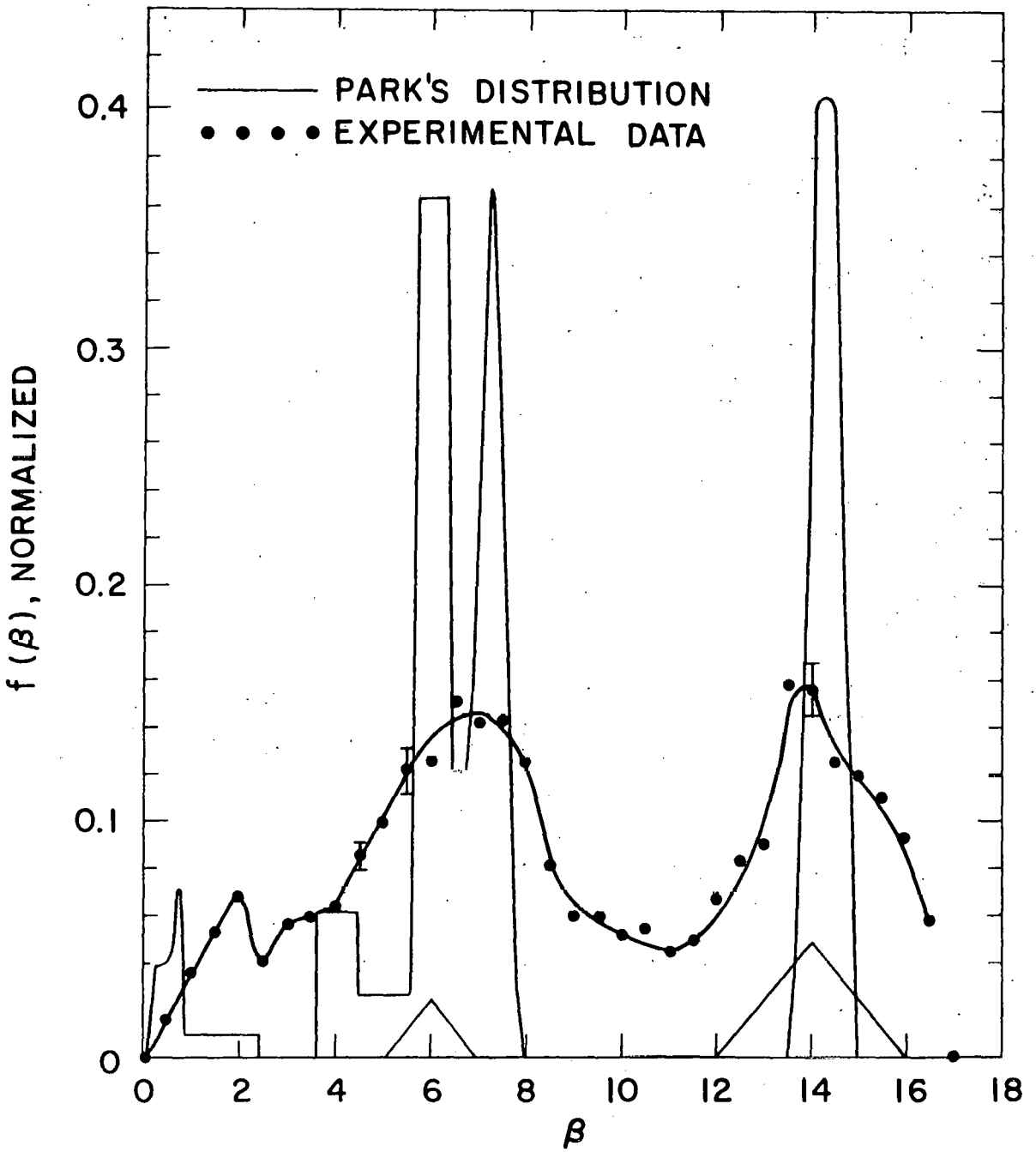

Fig. 20 --The frequency distribution f(β) derived from the generalized frequency distribution. Also shown for comparison purposes is the frequency distribution used by Parks for calculating the scattering cross section of polyethylene. The deltas at β = 6 and β = 14 represent estimated energy resolution

theory treated earlier (SUMMIT). Although the integrated value of $f(\beta)$ should be unity, the present data integrate to about 1.4 and attest to the difficulty of making meaningful extrapolations to $\alpha = 0$.

The contribution of higher-order phonon terms to the derived frequency distribution can be treated in various ways. For example, it can be minimized, as noted above, by making extrapolations only for $\alpha << 4$. This is impractical, however, when large incident energies are used. On the other hand, a correction for their contribution can be estimated by using the SUMMIT code to calculate individual contributions by each phonon term to either the scattering cross section or the Scattering Law. When this is done, one finds that the one-phonon term makes its major contribution to the scattering cross section (and hence, Scattering Law) only for non-zero values of the true frequency distribution. The contributions to the scattering cross section for other values of β come from the higher-order phonon terms. Unfortunately, for larger values of α, the higher-order phonon terms also make significant contributions in the non-zero region of $f(\beta)$ as well. Because of this latter fact and because all corrections in this instance are very large, it is of dubious value to attempt a further correction of the experimental frequency distribution obtained by the extrapolation method. It is of interest to note that the LEAP program[19] attempts to correct the generalized frequency distribution $p(\beta)$ for the contributions of the higher-order phonon terms. However, it would appear to be of limited value when the contribution from the higher-order phonon terms is as extensive as in the present case.

THIS PAGE

WAS INTENTIONALLY

LEFT BLANK

4. SOME CONSIDERATIONS OF NEUTRON SCATTERING IN GRAPHITE

At this writing, the experimental program on graphite has just been started, and only preliminary results are available. By the end of this contract year (nearly three months hence), the experimental situation should be much improved.

In other programs, experimental and theoretical results have been obtained for graphite, a coherent neutron scatterer. However, the experimental results have been obtained mostly from low incident neutron energies below 0.1 eV. In one case, Egelstaff[20] used cold neutrons scattered by a hot specimen of graphite (950°C) to study the higher-lying energies (up to 0.2 eV). In the earlier work, no effect on the higher levels was investigated because the sample was at ambient temperature and the incident neutron energy was less than 0.1 eV. Egelstaff's later work with cold neutrons revealed energy levels at about 0.08, 0.12, and 0.18 to 0.215 eV.

A rather complete theoretical treatment on graphite has been given by Wikner *et al.*[21] and Young and Koppel.[22] In their work, Young and Koppel predict energy levels at about 0.02, 0.056, 0.08, 0.108, 0.136, 0.155, and 0.175 up to about 0.21 eV, all surmounting a broad overlapping spectrum. Their results are shown in Figure 21. A discrepancy exists for the level at 0.108 eV compared with Egelstaff's level at 0.12 eV. This discrepancy is probably not due to coherent effects since, essentially, the data of Egelstaff were presented for constant momentum transfer.

In order to examine the scattering cross section with high energy neutrons in which a specimen at ambient temperature can be successfully used, we have employed the General Atomic neutron velocity selector to obtain neutrons with incident energies in the range of 0.15 to 0.3 eV. Preliminary scattering results are shown in Figures 22 and 23 for E_o = 0.170 and 0.227 eV, for scattering at 30 and 60 degs. Figure 22 shows evidence in the scattering cross section for levels around 0.055 and 0.085 eV, in agreement with predictions of Young and Koppel. The results in Figure 23 confirm the peak at about 0.085 eV and show a peak at 0.12 eV, together with a broad peak from 0.15 to 0.19 eV. In both Figure 22 and 23, we find a minimum in the scattering distribution at 0.11 eV where Koppel and Young predict a strong peak. The present results, together with Egelstaff's earlier data, indicate the possible need for theoretical attention to this predicted energy level.

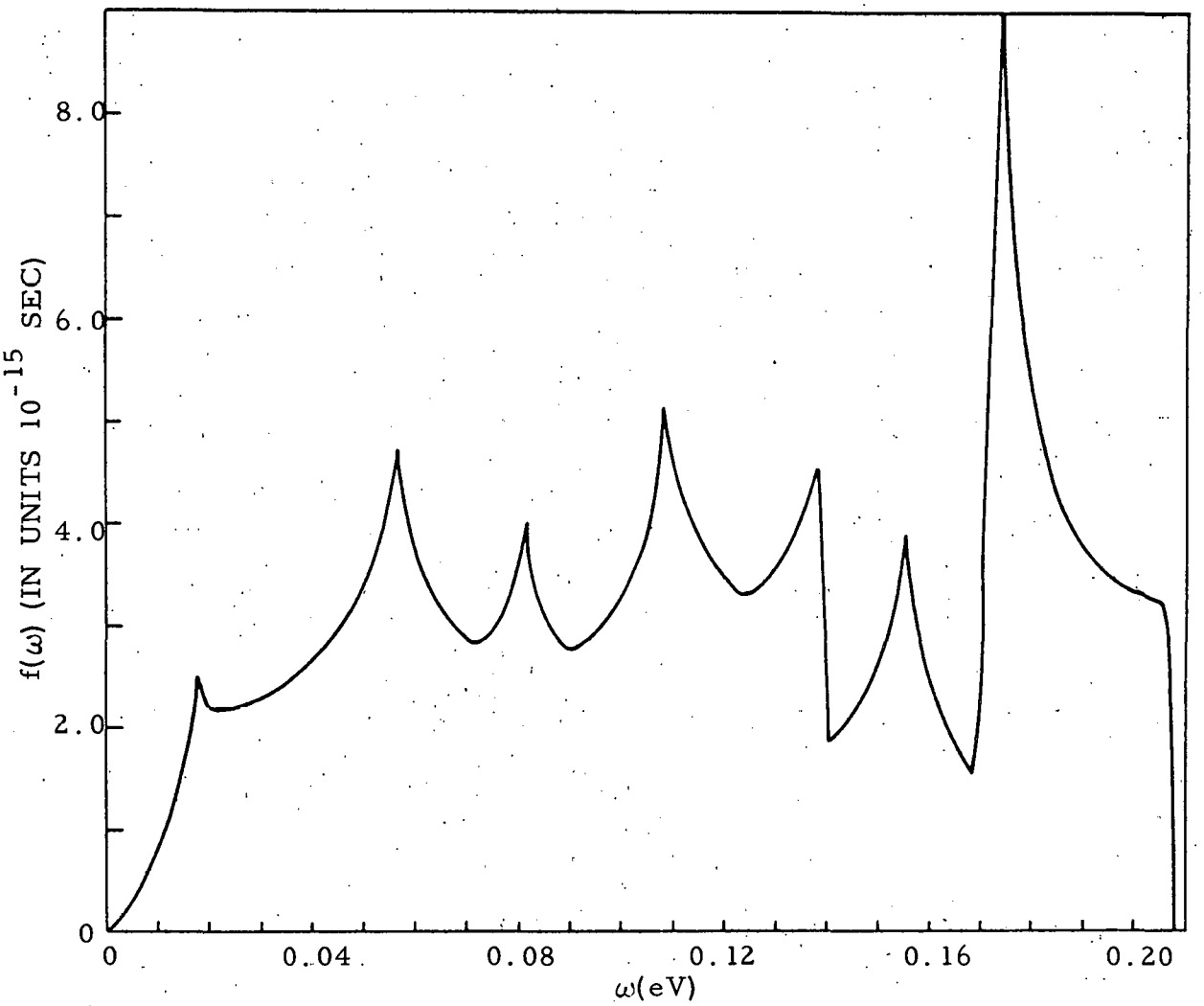

Fig. 21--Theoretical frequency spectrum $f(\omega)$ of reactor-type graphite. (From Young and Koppel, Ref. 22)

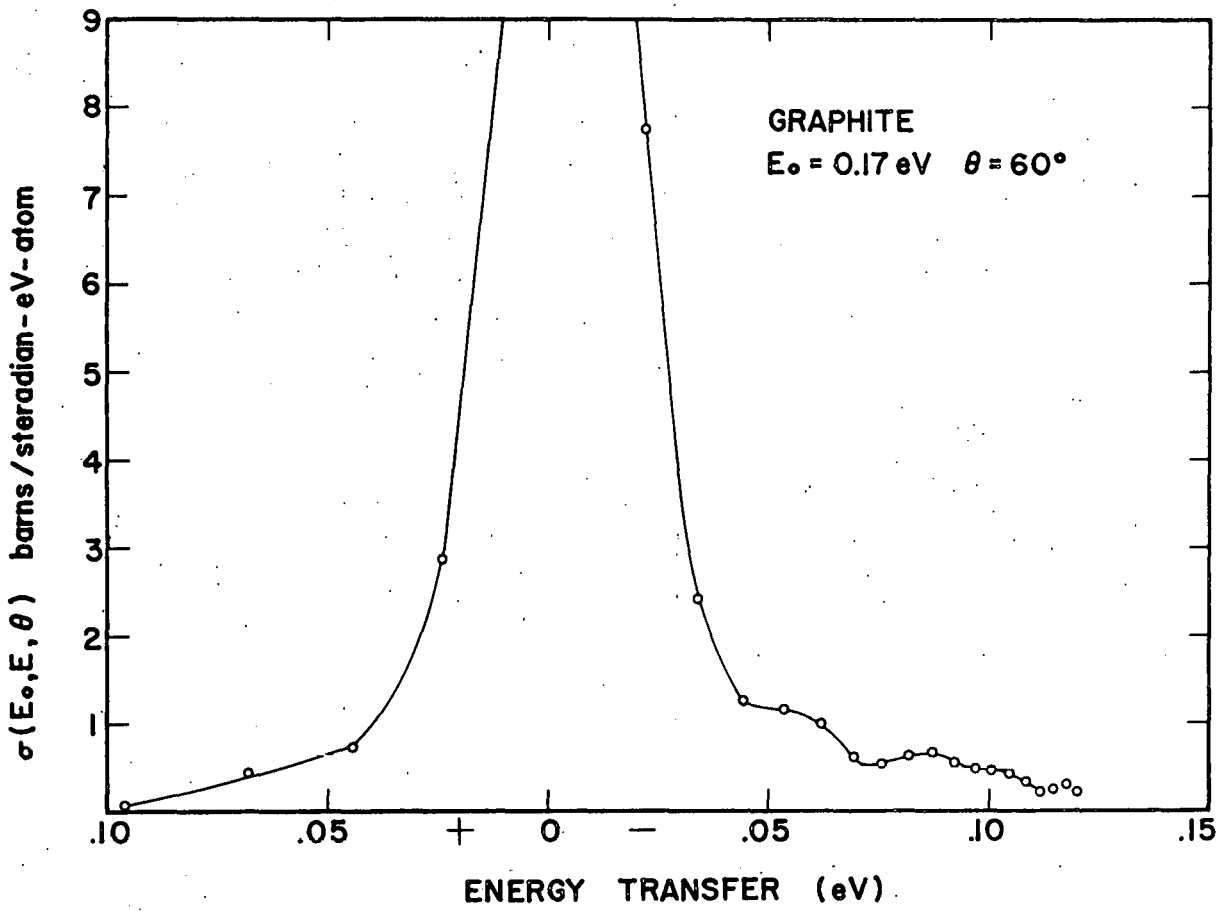

Fig. 22--Experimental scattering results on reactor grade graphite, using neutrons with E_o = 0.17 eV and a scattering angle of 60 deg

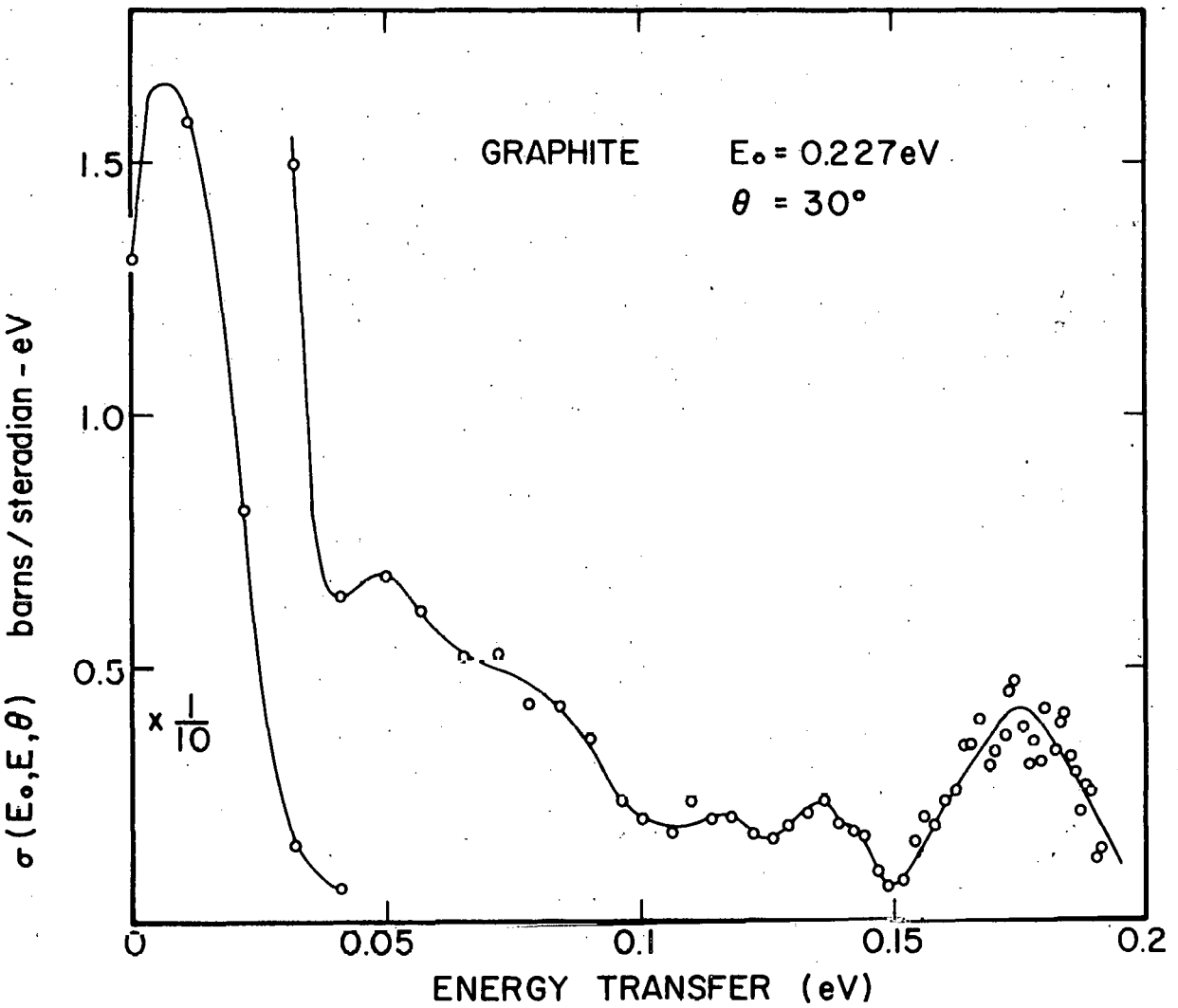

Fig. 23--Experimental scattering results on reactor grade graphite, using neutrons with E_o = 0.227 eV and a scattering angle of 30 deg

It is recognized that for energy transfers not corresponding to energy levels in the crystalline specimen, spurious peaks and structure in the energy-transfer cross section may occur for coherent scatterers. Such effects have already been indicated by the work of Schmunk[23] on beryllium and the work of Brugger and Randolph[24] on aluminum powder. Because our specimen of reactor type graphite is polycrystalline, it is necessary to consider these possible effects on the experimental measurements we have obtained so far.

In order to investigate the effects of coherent scattering on the results which we obtained experimentally, one must evaluate the appropriate reciprocal lattice vectors for the experimental cases at hand. Since we have a polycrystalline specimen, it is sufficient to calculate the magnitude of the pertinent reciprocal lattice vectors and list those which fall within the experimental range of momentum transfer for each measured case. Appropriate conclusions on the significance of the experimental data can then be generated.

An appropriate expression for the magnitude of the reciprocal lattice vector $|\vec{K}|$ in graphite is given as follows:

$$|\vec{K}| = 2\pi \left(\frac{2}{3a}\right) \left[\ell_1^{\,2} + \ell_2^{\,2} + \ell_3 \left(\frac{3a}{2a_3}\right)^2 - \frac{1}{2}\,\ell_1\ell_2\right]^{\frac{1}{2}} \qquad (13)$$

where a = lattice parameters = 1.42 Å,

$a_3 = 6.70$ Å,

and the ℓ_1's are integer indices describing the edges of the Brillouin zones. When evaluated, this expression reduces to the following (in units of $Å^{-1}$):

$$|\vec{K}| = 2.95 \left[\ell_1^{\,2} + \ell_2^{\,2} + 0.101\ \ell_3^{\,2} - \frac{1}{2}\,\ell_1\ell_2\right]^{\frac{1}{2}} .$$

Taking all possible combinations of ℓ_1 in this expression, we see that there are more than 700 possible values of reciprocal lattice vectors. By using a small computer program, we have evaluated the appropriate lattice vectors. Table VI lists the appropriate momentum transfer in units of $Å^{-1}$ and the experimental range around these values. In the last column, one finds the number of reciprocal lattice vectors which fall within this range. Examination of Table VI indicates that in almost every instance, a very large number of Bragg scattering planes contribute to the experimental data. From this, one comes to the conclusion that the "incoherent" approximation is probably valid for these experiments carried on with large energy incident neutrons. For this case, one would expect then that

TABLE VI

A Listing of the Range in Momentum Transfers for the Experimental Conditions and the Number N of the Relevant Reciprocal Lattice Vectors Lying in the Range ΔK

(E_o is the incident energy; ϵ is the energy transfer; θ is the scattering angle; $|K|$ is the absolute value of the momentum transfer; and $\Delta|K|$ is the range in momentum transfer corresponding to variations (experimental) in E_o, ϵ, and θ.)

E_o (eV)	ϵ (eV)	θ	$\lvert K\rvert$ (Å^{-1})	$\Delta\lvert K\rvert$ (Å^{-1})	N
0.170	0.120	30	5.40	0.204	20
		60	7.85	0.388	18
		90	10.29	0.428	16
		120	12.24	0.412	29
		150	13.51	0.312	0
0.170	0.090	30	4.82	0.291	8
		60	8.04	0.478	28
		90	10.98	0.504	17
		120	13.25	0.475	24
		150	14.17	0.355	0
0.170	0.050	30	4.53	0.498	48
		60	8.04	0.478	28
		90	10.98	0.504	17
		120	13.25	0.475	24
		150	14.17	0.355	0
0.229	0.120	30	6.74	0.187	20
		60	9.12	0.412	10
		90	11.60	0.485	36
		120	13.60	0.492	0
		150	15.02	0.400	0
0.229	0.090	30	6.00	0.272	8
		60	9.15	0.506	20
		90	12.18	0.558	43
		120	14.60	0.545	0
		150	16.18	0.426	0
0.229	0.050	30	5.47	0.371	32
		60	9.41	0.608	20
		90	12.95	0.650	54
		120	15.80	0.626	0
		150	17.50	0.489	8

the evidence for energy levels in the crystal would appear at all scattering angles at the same energy transfer. Indeed this is the case, as examination of the existing experimental data confirms.

Although analysis of the data is still continuing, some information exists for higher energy incident neutrons. Figure 24 shows a typical energy transfer plot of experimental data for neutrons with 0.316 eV incident energy. This particular energy was chosen to give information on the higher energy levels in graphite and, in particular, some information on the high energy cutoff. The work of Young and Koppel[22] indicates that the upper cutoff should be about 0.21 eV. The experimental curve shows structure in the energy transfer cross section in the range 0.20 to 0.22. The cutoff shown in the curve appears at ~0.23 to 0.24 eV. Allowance must be made for the effect of energy resolution of the apparatus. For energy transfers of ~0.21 eV, with an incident energy of 0.316 eV, one computes that the energy resolution is about $(\Delta E)_{calc} = 0.047$. This is sufficient to broaden a cutoff at 0.21 eV to ≃0.235 eV. At the present time, one must say that the cutoff is consistent with that value predicted by Young and Koppel. Additional analysis of the existing experimental information and additional experimental measurements will be needed to clarify this particular point.

In conclusion, it appears that additional experimental information on these various points is warranted and will be useful in clarifying certain features of the predicted frequency distribution and matters of neutron moderation in graphite.

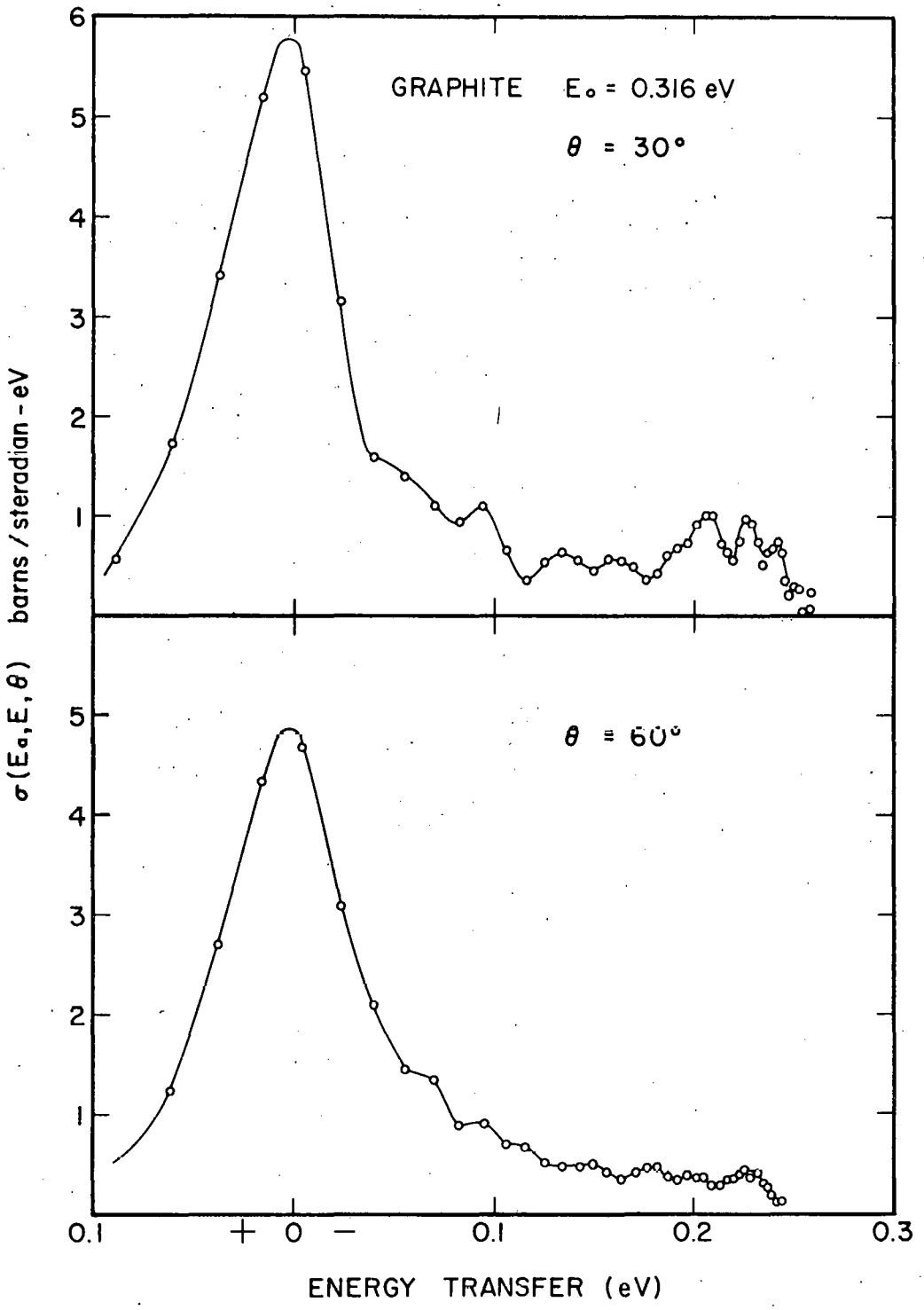

Fig. 24--Neutron inelastic scattering by reactor grade graphite. θ = 30 and 60 deg. Neutron incident energy was 0.316 eV.

5. RESULTS ON SCATTERING OF NEUTRONS BY LIQUID METHANE

Since intense pulsed sources of cold neutrons from reactors are improved through the use of cold thermalizers and since our previous experimental results[3] have indicated that liquid methane is a useful candidate, we have made an experimental run with a thin scattering sample of liquid CH_4 to gain additional pertinent information on these matters. A high incident energy was chosen in an effort to provide experimental data for checking the theoretical calculations in a region not previously tested. McMurry[25] at Phillips has provided some theoretical calculations for large angle scattering of neutrons with this high neutron energy, using techniques described elsewhere.[26-28]

McMurry has pointed out that some work of Brugger indicates that computational methods for calculating the contributions of vibrational excitations are not completely accurate. The present experiment is intended to provide information on this point. Measurements have been made at large scattering angles so that the contribution of the carbon atom scattering would be clearly separated from that due to excitational and vibrational levels. The data in Figure 25 shows the experimental and theoretical results obtained at a typical large scattering angle. The experimental results are provisional as regards absolute cross section since the scattering sample thickness was not known with precision. The shape of the experimental curve for large energy transfers differs significantly from the theoretical curve. In particular, the cross sections of final energy states around 0.08 to 0.10 eV differ in that more structure is observed in the experimental curve than predicted by the theory. A repetition of the experiment will be made to confirm that the result is valid and not caused by spurious effects in the sample holder. Tentatively, however, one is led to the conclusion that the theoretical treatment may overlook certain fundamental characteristics of neutron scattering by liquid methane.

McMurry has used different methods of computation of the averages over molecular orientations. The calculations, without the exact averaging over molecular orientation used in Figure 25 and illustrated in greater detail in Figure 26, are based on a model that assumes that rotational motions can be treated classically, that vibrations can be considered harmonic, and that the interaction between rotation and vibration coupling can be neglected. These seem to be quite reasonable assumptions for a semi-rigid molecule like CH_4, for the large energy exchanges contemplated

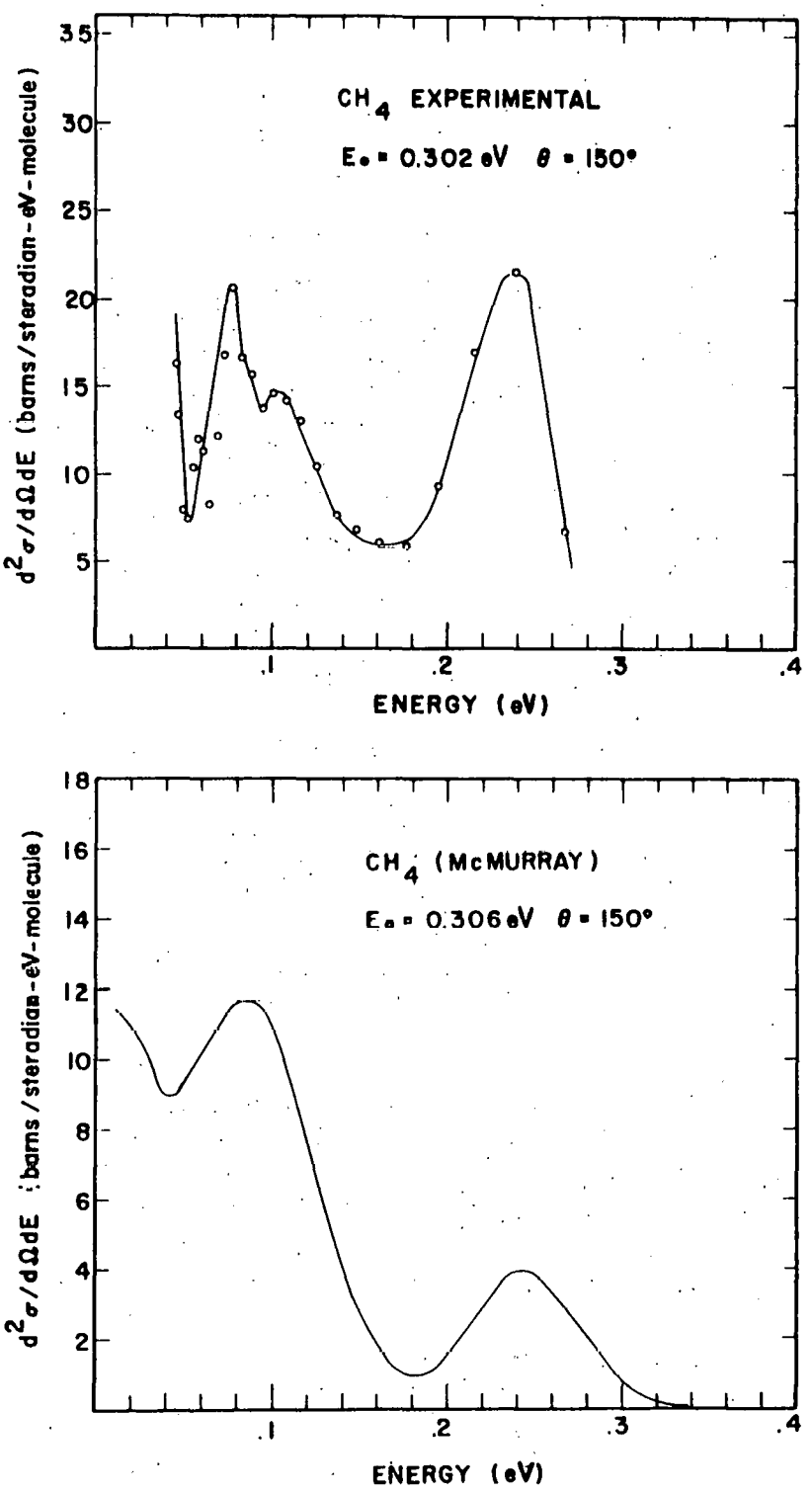

Fig. 25--Experimental and theoretical results obtained at a typical large scattering angle (150 deg).

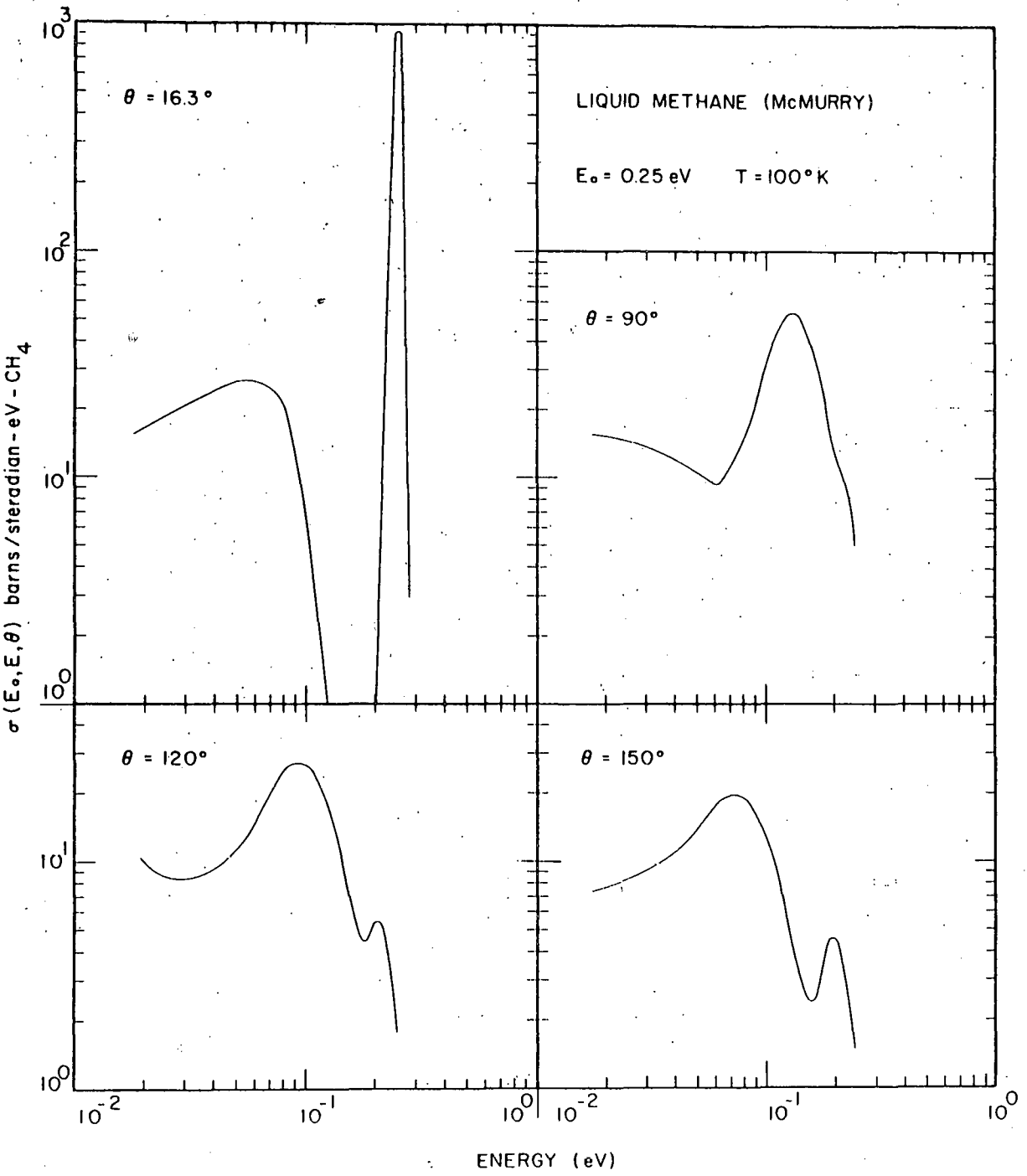

Fig. 26--Computed cross section for E_o = 0.25 eV of McMurry for liquid methane at 100°K

in the present experiments. However, it has been suggested that rotation-vibration coupling might produce sizeable effects in the experimental domain under consideration. It has further been pointed out that an impulsive scattering interaction with rapid particle recoil might involve conditions where the Born-Oppenheimer separation is not valid. The calculated intensities which result from an exact average over molecular orientation are somewhat larger than when the calculation is made without averaging, but the increase is not enough to resolve the discrepancies between the theory (without exact averaging) and experiment as shown in Figure 25. Of perhaps greater importance is the fact that exact averaging washes out some of the structure present when the Krieger-Nelkin procedure for averaging is used. At present it appears that theory and experiment are somewhat different for neutron scattering at large angles for large neutron incident energies. Before serious additional theoretical calculations are contemplated, it seems entirely reasonable to render reasonably precise the experimental situation. It is our intention during the continuing neutron differential-scattering program to provide such additional experimental information on liquid methane.

6. CONSIDERATION OF LEVEL WIDTHS IN METAL HYDRIDES

Inelastic scattering of neutrons has been studied for various metal hydrides. An earlier report[4] presented some of the time-of-flight distributions. Some of these data have been processed by the CROSEC program to give cross section data. Figures 27 and 28 illustrate the results for the yttrium hydrides, $YH_{1.87}$ and $YH_{2.50}$. One sees that a sharply bound level appears in the specimen of $YH_{1.87}$, whereas such evidence is lacking for $YH_{2.5}$. The sharp energy level $h\nu$ in $YH_{1.87}$ has a value of about 0.122 eV. Lack of a single sharp energy level in $YH_{2.5}$ is presumably related to a change in lattice structure with the increased content of hydrogen. In a study of a hydride with similar structure, holmium hydride, Mansmann and Wallace[29] elaborate on several details of interest which help to explain the disappearance of the sharp level in yttrium hydride. Presumably, the explanation lies in changes in lattice structure which introduce other modes of hydrogen binding with lower frequencies. A change of lattice symmetry would also remove the triple degeneracy of the Einstein level. The result for the higher hydride would be to create as many as six frequencies in place of the single one. Such an explanation is consistent with the result observed in Figure 28, though evidence for all the frequencies is not seen.

Data on neutron scattering for metal hydrides, accumulated earlier in this program, has been further analyzed in order to derive better estimates of their energy-level widths. Some information on level widths for zirconium hydride has been presented in earlier publications.[4, 19] This information has been revised, using a refined computational technique, and additional data are now presented.

As mentioned earlier in this report (Section 2) and in previous reports,[4] a computer program permits one to compute the expected width of an experimentally observed level, taking into account the experimental resolution effects. It also allows one to take into account, as needed, the finite width of the level giving rise to the inelastically scattered neutrons. If the natural width is taken as zero, the predicted width represents the resolution of the apparatus. Such values, called $(\Delta E)_{calc}$, have been tabulated in Tables I and II in Section 2. Use of the program allows one to search for that natural width of the level which creates agreement between the predicted and observed time-of-flight distributions.

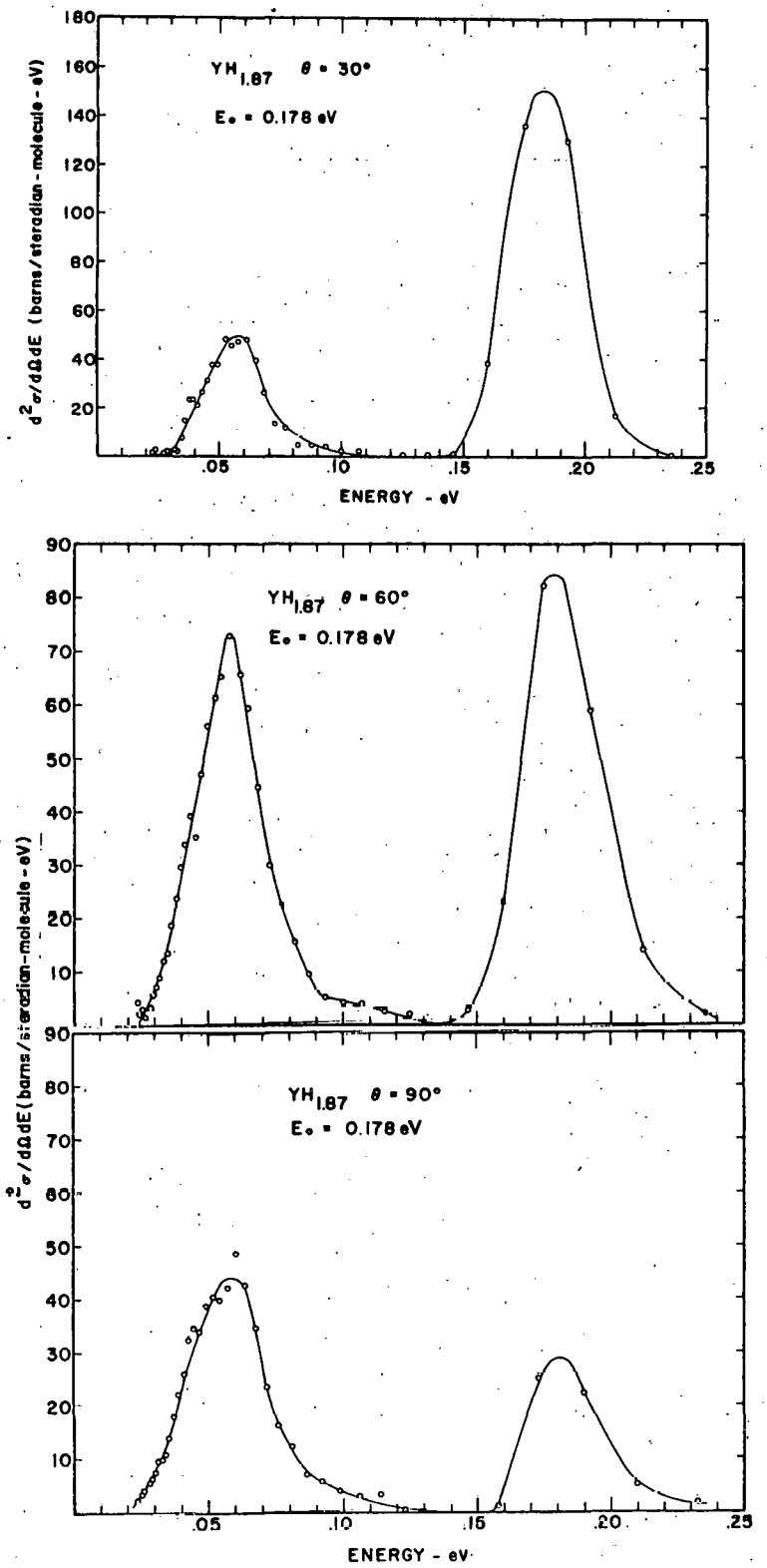

Fig. 27--Inelastic scattering of 0.178 eV neutrons by $YH_{1.87}$ at 30, 60, and 90 deg

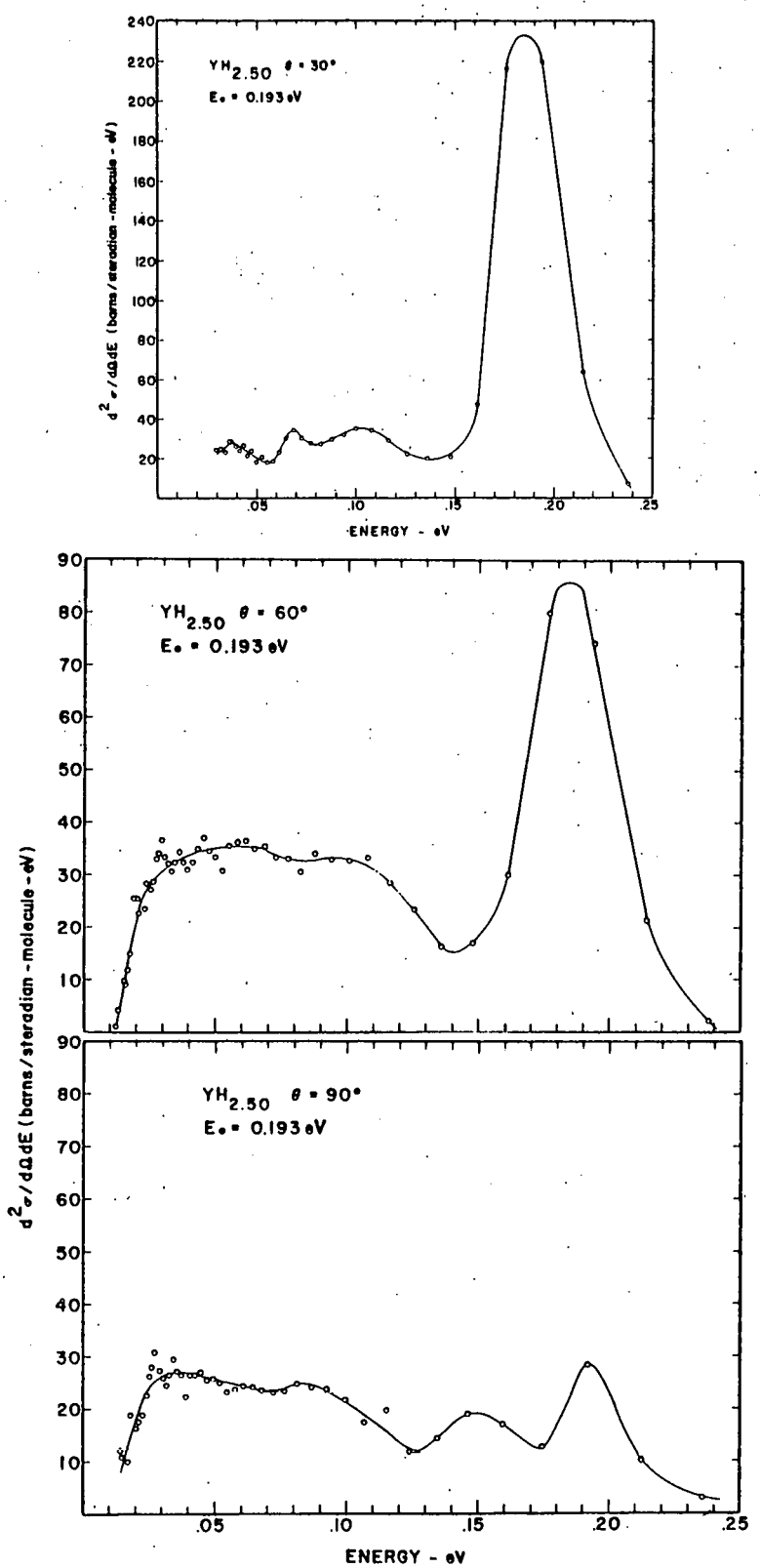

Fig. 28--Inelastic scattering of 0.193 eV neutrons by $YH_{2.50}$ at 30, 60, and 90 deg

With the previous method, the measured widths of sharp levels in some metal hydrides have been corrected for effects of instrumental resolution. The resulting level widths are shown in Table VII. There appears to be some dependence of level width on the sample temperature in the range 90°K to 300°K.

TABLE VII

Einstein Levels $h\nu$ in Several Metal Hydrides and the Associated Level Widths $\Delta h\nu$ (FWHM)

Hydride	$h\nu$ (eV)	$\Delta h\nu$ (eV)
$ZrH_{2.0}$ (300°K)	0.140	0.016
$ZrH_{2.0}$ (90°K)	0.140	0.009
$YH_{1.87}$	0.122	0.015
$LaH_{2.0}$	0.103	0.003

It is recognized that the change with temperature of zirconium hydride is somewhat larger than previously reported.[3,17] This is due to the new computational procedure which revises the predicted level widths downward and attributes more significance to the small but measureable differences in the observed level widths.

The data reported in Table VII and discussed briefly above are being subjected to further scrutiny. These data were accumulated earlier in the program, using high energy incident neutrons. The instrumental resolution was not known in this earlier period with as much precision as desirable. The relative comparison of these data listed here is believed to be reliable. However, as a check on these level widths, repeated runs with the present apparatus, which has twice the experimental resolution, would be highly useful and desirable.

One can speculate on the relation of the widths for the first and higher bound levels in a single metal hydride. In earlier publications,[3,17] we made some preliminary comparisons of the first and second level widths

in zirconium hydride. We found it difficult to measure the width of the second level with precision. However, it appeared that the width of the second level was consistent with being $\sqrt{2}$ times the width of the first level. The improved estimates of resolution are being applied to these calculations but are not yet available. At this point, we would like to present the theoretical considerations which underlie the factor $\sqrt{2}$ connecting the widths of the first and second bound levels.

In the so-called harmonic approximation ("phonon" expansion) the scattering law $S_j(\kappa, \omega)$ is given[30] as follows:

$$S_j(\kappa, \omega) = \left[\exp\left(\frac{-\hbar\kappa^2}{2M_j}\ \alpha_j\right)\right]\left[\sum_{n=0}^{\infty} \frac{1}{n!}\left(\frac{\hbar\kappa^2}{2M_j}\ \alpha_j\right)^n \quad G_{jn}(\omega)\right] \quad , \tag{14}$$

where

$$G_n(\omega) = \int_{-\infty}^{\infty} G_1(\omega')\ G_{n-1}(\omega-\omega')d\omega' \quad . \tag{15}$$

It is seen that if G_1 is gaussean, then G_2 will also be gaussean since it is convoluted with itself. One concludes from this that if the first level can be represented fairly well by a gaussean distribution, then the second level will be $\sqrt{2}$ broader. The accuracy of this representation depends on the degree to which the first level is gaussean in shape.

Table VIII has been prepared to compare the results of Whittemore,[3,4,30] Leonard et al.,[32] Pan et al.,[33] and Woods et al.[34] Included in Table VIII are some pertinent experimental parameters, such as the final neutron energy and the values of the sample cross section, which significantly affect the sample transmission. The effect of multiple scattering can be inferred from the quantities indicated by the columns for $T(E_o)$ and $T(E_f)/T(E_o)$. For Leonard's results, one can only guess at the sample thickness used. We have used as typical values, $T = 0.8$ and $T = 0.9$. In general, multiple scattering effects are minimized by values of $T(E_o)$ and $T(E_f)/T(E_o)$ which both approach unity. It will be observed that the General Atomic results most nearly satisfy these conditions. It should be observed as well that these conditions affect $\Delta\hbar\omega$ (1) independent of the precision of the individual neutron energy determination of E_o and E_f.

TABLE VIII

Comparison of Various Widths of $\hbar\omega$ (1) for Zirconium Hydride and Related Experimental Parameters

Experimenter	$\Delta\hbar\omega$ (1) eV	E_o eV	$\bar{E}_f$ eV	$\sigma_H(E_o)$ barn	$\sigma(\bar{E}_f)$ barn	$T(E_o)$	$T(E_f)$	$\frac{T(E_f)}{T(E_o)}$
Whittemore	0.018	0.239	0.100	22	26	0.90	0.89	0.99
Leonard et al.	0.027 ± 0.001	0.180	0.040	26	47	[0.90]* [0.80]*	[0.82]* [0.67]*	[0.91]* [0.84]*
Woods et al.	0.025 - 0.027**	0.145	0-0.005	23	>78	0.70	<0.29	<0.41
Pan et al.	0.025	0.145	0-0.005	23	>78	0.80	<0.46	<0.58

* [ ] indicates pure assumption since Leonard et al. have not published any information on sample thickness or transmission.

** Taken from the published curve. (See Ref. 32.)

Let us consider the effect on $\Delta\hbar\omega$ (1) of experimental conditions which result in $T(E_f) << T(E_o)$. In Table VIII, it can be seen that the filter technique first used by Woods et al.,[34] satisfies these conditions. Assume for the moment that $\hbar\omega$ (1) is a line with no width [$\Delta\hbar\omega$ (1) = 0], that the energy determinations can be made without error ($\Delta E_o = \Delta E_f = 0$), and that there is no multiple scattering. For incident neutrons with $E_o < 0.140$, no energy transfers are possible since $(E_o - E_f) < \hbar\omega$ (1). Using a filter transmitting neutrons with energy from 0 to 0.005 eV, incident neutrons with energies in the range $\hbar\omega$ (1) to $\hbar\omega$ (1) + 0.005 eV will be inelastically scattered and will be detected through the filter. Thus the line $\hbar\omega$ appears to be broadened by ~0.005 eV. Let us now admit a large amount of multiple scattering of the neutron after it loses an energy $h\nu$. Although the energy after the first inelastic scatter may be in the range 0 to 0.005 eV, multiple scatter by the acoustic modes rapidly brings E_f to $\simeq kT$. Only that portion of the spectrum which now falls below 0.005 eV will be detected. Due to the same considerations, neutrons with incident energies E_o larger than $\hbar\omega$ (1) by $\simeq kT$ will also make a similar contribution to the flux of $E_f < 0.005$ eV. Thus the line exhibited by the filter technique and having a large amount of scattering of the low energy neutrons will be broadened artificially on the high energy side by $\simeq kT$, even if the original line has no width.

Now the multiple scattering in the experiment of Woods et al.,[34] was not large enough to thermalize the low energy neutrons completely; nevertheless, a thickness giving $T < 0.29$ approaches this condition. Therefore, due to these various effects, the value $\Delta\hbar\omega$ (1) $\cong$ 0.027 eV of Woods must be decreased. By the same token, the value of $\Delta\hbar\omega$ (1) of Pan et al.,[33] must be decreased, although the correction in this case should be smaller since a) below 0.005 eV, a different filter technique was used to decrease the effective filter width and b) the effective thickness for the low-energy neutrons was a little "thinner" than that used by Woods (see Table VIII). The data of Leonard et al.,[32] should require still less correction than that of either Pan or Woods, though some correction due to the above effect is surely required for neutrons with final energy of ~0.04 eV.

Theorists have attributed some significance to the skew shape of the first level in zirconium reported by Woods et al.[34] In view of the above considerations of multiple scattering which have the effect of artificially broadening the observed level on the high energy side, care should be exercised in this matter.

THIS PAGE

WAS INTENTIONALLY

LEFT BLANK

7. SOME CONSIDERATIONS OF OH AND CH VIBRATIONS

In the course of the extended research in this program, several opportunities have arisen to measure high energy molecular vibrations. In light water, the highest of these is caused by the motion of the H atom as it vibrates with respect to the OH group. Depending on whether a symmetric or antisymmetric motion is considered, the energy of this level is 0.474 or 0.480 eV. In heavy water, a similar situation pertains to the motion of D with respect to the OD group. The respective frequencies are expected to be roughly $\sqrt{2}$ smaller because of the change in mass. Similar high-energy vibrational levels exist for H-CH motion in polyethylene. The work of Lin and Koenig[15] indicates that this level should occur at about 0.35 eV.

Measurements made with the General Atomic Neutron Velocity Selector on specimens of polyethylene and heavy water may throw some additional light on the motion of tightly bound H and D atoms. Figure 29 shows an energy transfer plot for scattering by dense, highly crystalline CH_2, using neutrons with incident energy of 0.499 eV. This has been previously treated in Section 3.3. The apparent width of the level at $\epsilon = 0.35$ eV is almost entirely instrumental. The true, fundamental width is very narrow. Figure 30 shows an energy level centered on $\epsilon = 0.334$ eV for scattering by D_2O, using neutrons with incident energy of 0.404 eV. The apparent width of this level is also mostly due to instrumental resolution effects. The true width is thus very narrow. The transfer energy 0.334 eV in D_2O is smaller than the similar level in H_2O by a factor of almost exactly $\sqrt{2}$, as discussed above.

The above experimental data verify the expectation that the high frequency vibrational levels are very sharp in CH_2 and D_2O. It will be useful to repeat these measurements with improved instrumental resolution to determine with precision the exact width of these vibrational levels.

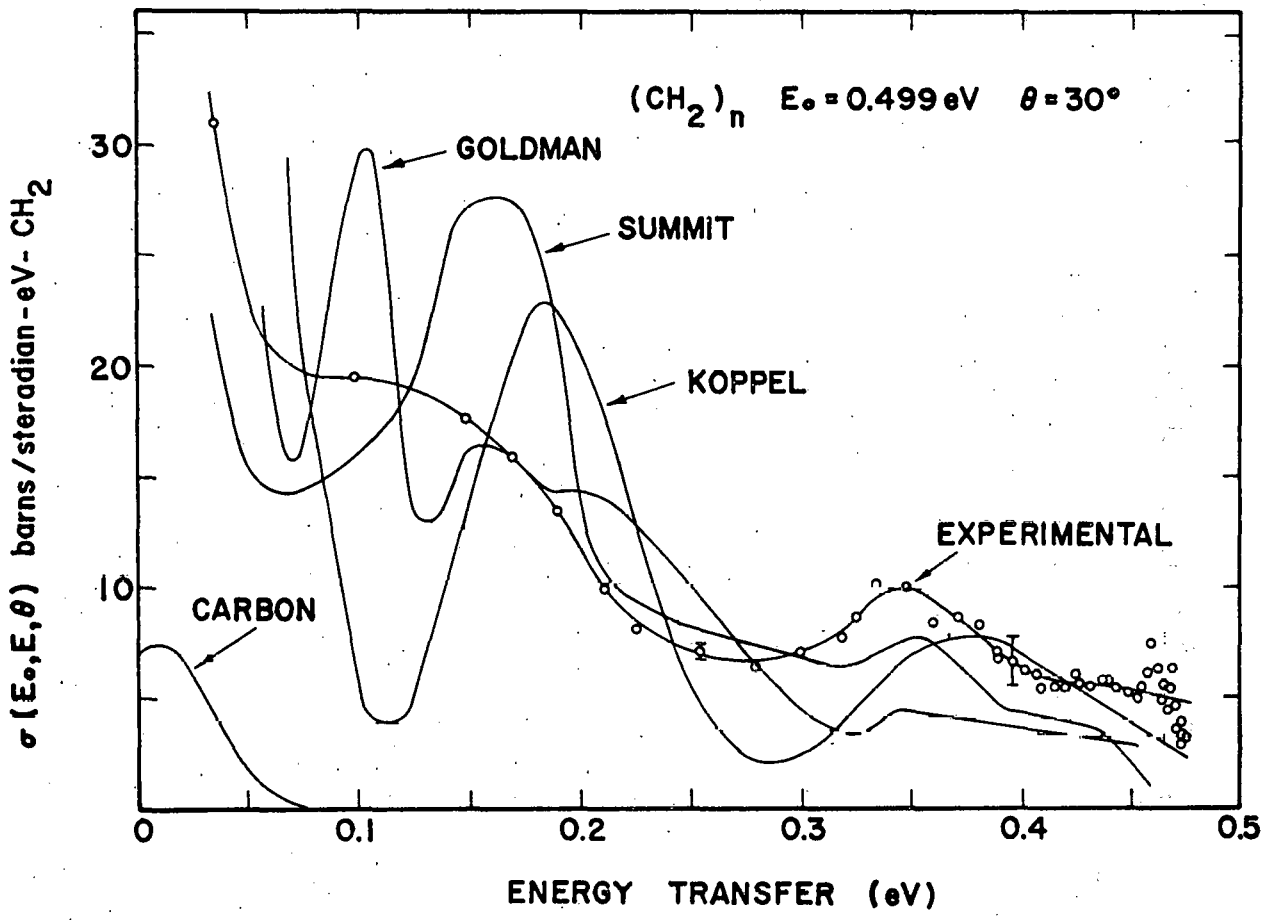

Fig. 29--Scattering cross section of crystalline polyethylene observed at 30 deg, using 0.499 eV neutrons. Theoretical results are also indicated

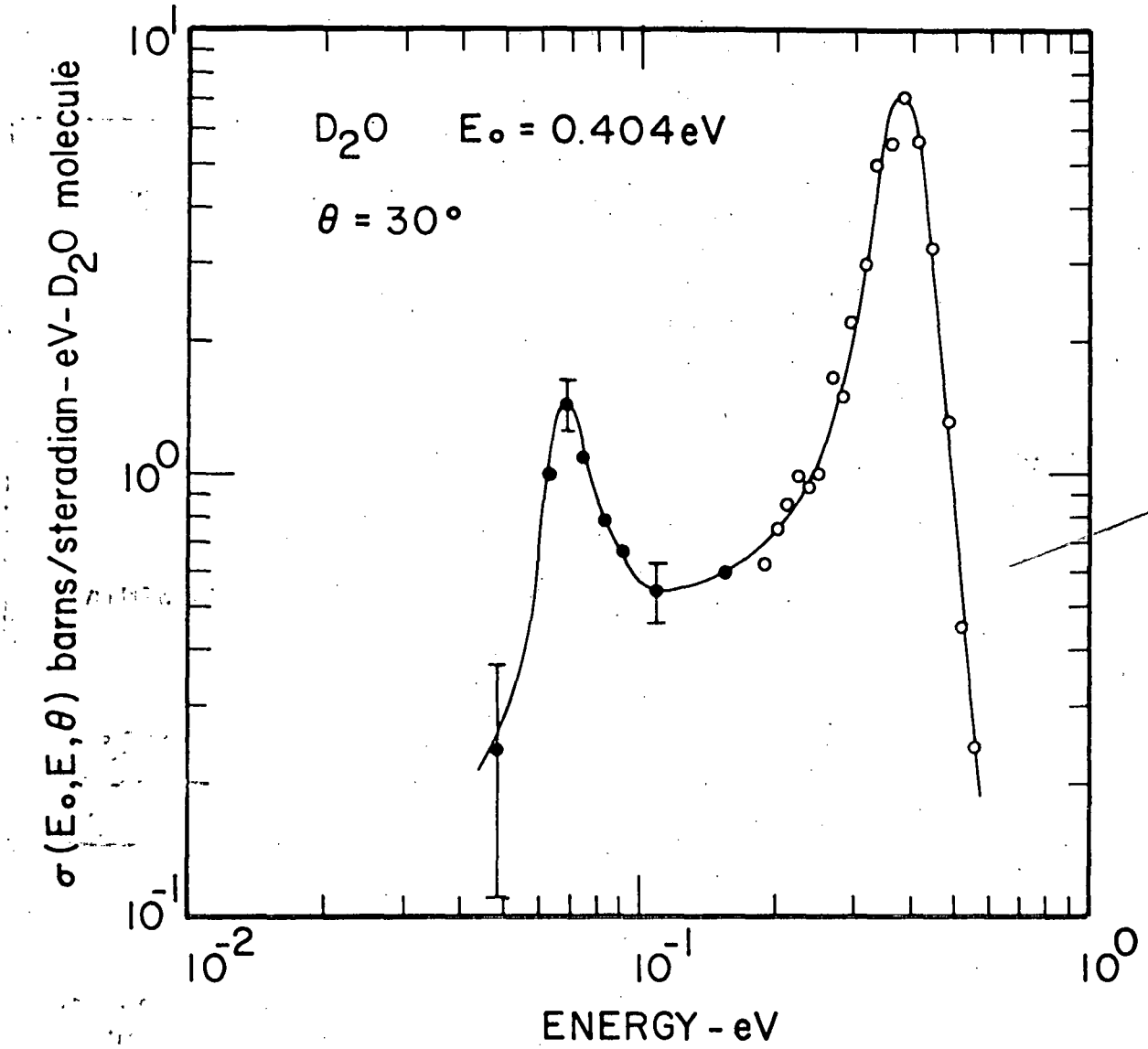

Fig. 30--Differential scattering by D_2O at 30 deg for neutrons with energy of 0.404 eV

THIS PAGE

WAS INTENTIONALLY

LEFT BLANK

REFERENCES

1. Whittemore, W. L., Differential Neutron Thermalization, Annual Summary report covering the period October 1, 1960 through September 30, 1961, on Contract AT(04-3)-167, P.A. 10, USAEC report GA-2503 (General Atomic Division, General Dynamics Corporation, San Diego, California, 1961).

2. Whittemore, W. L., Differential Neutron Thermalization, Annual Summary report covering the period October 1, 1961 through September 30, 1962, on Contract AT(04-3)-167, P.A. 10, USAEC report GA-3409 (General Atomic Division, General Dynamics Corporation, San Diego, California, 1962).

3. Whittemore, W. L., Differential Neutron Thermalization, Annual Summary report covering the period October 1, 1962 through September 30, 1963, on Contract AT(04-3)-167, P.A. 10, USAEC report GA-4434 (General Atomic Division, General Dynamics Corporation, San Diego, California, 1963).

4. Whittemore, W. L., Differential Neutron Thermalization, Annual Summary report covering the period October 1, 1963 through September 30, 1964, on Contract AT(04-3)-167, P.A. 10, USAEC report GA-5554 (General Atomic Division, General Dynamics Corporation, San Diego, California, 1964).

5. Kottwitz, D. A., B. R. Leonard, "Quasi-Elastic Scattering by Room Temperature Light Water," in Inelastic Scattering of Neutrons in Solids and Liquids, proceedings of symposium at Chalk River, September 10-14, 1962, sponsored by the International Atomic Energy Agency. (IAEA, Vienna, Austria, 1963).

6. Smith, C. V., TPLOT and ICON - Two General-Purpose Plotter Codes for Use with the SC 4020, report number GAMD-4346 (Rev.), (General Atomic Division, General Dynamics Corporation, San Diego, California, 1964).

REFERENCES (Cont.)

7. Goldman, D. T., and F. D. Federighi, in Inelastic Scattering of Neutrons in Solids and Liquids, proceedings of symposium at Chalk River, September 10-14, 1962, sponsored by the International Atomic Energy Agency (IAEA, Vienna, Austria, 1963), Vol. I, pp. 389-404. Also, Nucl. Sci. Eng. 16, 165 (1963).

8. Parks, D., in Integral Neutron Thermalization, by J. R. Beyster et al., Annual Summary report for October 1, 1962 through September 30, 1963, on Contract AT(04-3)-167, P. A. 2, USAEC report GA-4659 (General Atomic Division, General Dynamics Corporation, San Diego, California, 1964), Sec. IV, pp. 79-84.

9. Nelkin, M., Phys. Rev. 119, 741 (1960).

10. Koppel, J. U., and J. A. Young, Nucl. Sci. Eng. 21, 268 (1965).

11. Matthews, J. R., H. S. Peiser, and R. B. Richards, Acta Cryst, 2, 85 (1949).

12. Kirouac, G. J., W. E. Moore, K. W. Seeman, and M. L. Yeater, Linear Accelerator Quarterly Project Report, for October through December 1964, on Contract AT(30-3)-328, (Rensselaer Polytechnic Institute, Troy, New York, 1964).

13. Koppel, J. U., and J. A. Young, in Integral Neutron Thermalization, by J. R. Beyster et al., Quarterly report for period ending December 31, 1964, on Contract AT(04-3)-167, P. A. 2, USAEC report GA-6096 (General Atomic Division, General Dynamics Corporation, San Diego, California, 1965), Sec. IV. 3, pp. 29-40.

14. Wunderlich, B., J. Chem. Phys. 37, 1207 (1962).

15. Lin, T. P., and J. L. Koenig, J. Molec. Spectr. 9, 228 (1962).

16. Parks, D., M. Nelkin, N. F. Wikner, and J. Beyster, A Book on Slow Neutron Scattering and Neutron Thermalization, Sponsored and to be published by USAEC, 1965, (CH. II).

REFERENCES (Cont.)

17. Whittemore, W. L., The Nature of Hydrogen Motion in ZrH Determined from an Experimental Neutron Study of Large, Bound Energy Levels, report number GA-5744 (General Atomic Division, General Dynamics Corporation, San Diego, California, 1964). (To be published in IAEA Proceedings for the Symposium on Inelastic Scattering of Neutrons in Solids and Liquids held in Bombay, India, December 1964).

18. Egelstaff, P. A., "The Theory of the Thermal-Neutron Scattering Law," in Inelastic Scattering of Neutrons in Solids and Liquids, proceedings of symposium at Vienna, 1960, sponsored by the International Atomic Energy Agency. (IAEA, Vienna, Austria, 1961), Vol. I. pp. 25-37.

19. Macdougall, J. D., in Proceedings of the Brookhaven Conference on Neutron Thermalization, (Brookhaven National Laboratory, Upton, Long Island, New York, 1962), Vol. I, pp. 121-143.

20. Egelstaff, P., and D. Harris, Phys. Letters 7, 220 (1963).

21. Wikner, F., G. Joanou, and D. Parks, Nucl. Sci. Eng. 19, 108 (1964).

22. Young, J., and J. Koppel, J. Chem. Phys. 42, 357-64 (1965).

23. Schmunk, R. E., Phys. Rev. 134, A1303 (1964).

24. Brugger, R. M., and P. D. Randolph, Slow Neutron Inelastic Scattering from Aluminum Powder, report number IDO-17063, on Contract AT(10-1)-205, (Phillips Petroleum Company, Atomic Energy Division, Idaho Falls, Idaho, 1965).

25. McMurry, H. L., NRTS Idaho (private communication).

26. McMurry, H. L., L. J. Gannon, W. A. Hestir, Nucl. Sci. Eng. 15, 438 (1963).

27. McMurry, H. L., G. W. Griffing, W. A. Hestir, and L. J. Gannon, An Evaluation of the Krieger-Nelkin Method from Calculations of Slow Neutron Scattering by CH_4, report number IDO-16692, on Contract AT(10-1)-205, (Phillips Petroleum Company, Atomic Energy Commission, Idaho Operations Office, 1961).

REFERENCES (Cont.)

28. McMurry, H. L., L. H. Gannon, A Machine Program for Calculating Slow Neutron Scattering Cross Section with Application to Water, report number IDO-16984, on Contract AT(10-1)-205, (Phillips Petroleum Company, Atomic Energy Division, Idaho Falls, Idaho, 1964).

29. Mansmann, M., and W. E. Wallace, J. de Physique, 25, 454 (1964).

30. Whittemore, W. L. Neutron Interactions in Zirconium Hydride, report number GA-4490 (Rev.) (General Atomic Division, General Dynamics Corporation, San Diego, California, 1964.)

31. Parks, D., M. Nelkin, N. F. Wikner, and J. Beyster, A Book on Slow Neutron Scattering and Neutron Thermalization, Sponsored and to be published by USAEC, 1965, (Ch. III).

32. Leonard, B. R., and O. K. Harling, Bull. Am. Phys. Soc. 10, 436 (1965).

33. Pan, S. S., M. L. Yeater, F. Bischoff, and W. A. Bryant, The Inelastic Scattering of Low-Energy Neutrons by Zirconium Hydride-1.37, Thorium Hydride and Niobium Hydride, Linear Accelerator Project Progress Report, October through December, report number RPI-328-20 (Rensselaer Polytechnic Institute, Troy, New York, 1964), pp. 35-39.

34. Woods, A. D. B., B. N. Brockhouse, M. Sakamoto, and R. N. Sinclair, "Energy Distributions of Neutrons Scattered from Graphite, Light and Heavy Water, Ice, Zirconium Hydride, Lithium Hydride, Sodium Hydride, and Ammonium Chloride by the Beryllium Detector Method," in Inelastic Scattering of Neutrons in Solids and Liquids, proceedings of the Symposium at Vienna, October 11-14, 1960, sponsored by the International Atomic Energy Agency, (IAEA, Vienna, Austria, 1961) pp. 487-498.

APPENDIX I

X-RAY ANALYSIS OF THIN $(CH_2)_n$ SPECIMENS FOR AMORPHOUS CONTENT

A technique for x-ray analysis of thin specimens of polyethylene developed by Matthews et al[11] has been applied to the two samples used in the present studies of neutron inelastic scattering. One was a high density (0.963 gm/cc) specimen prepared by Monsanto Corporation. The other was a low density (0.920 gm/cc) specimen. The x-ray results are shown in Figure 31. The peak at 4.496 Å indicates the amorphous content in the sample. Analysis of the x-ray scattering patterns in the manner of Matthews yields an amorphous content of less than 10 percent for the Monsanto sample and approximately 40 percent in the low density sample. These data are consistent with the sample density according to Matthews.

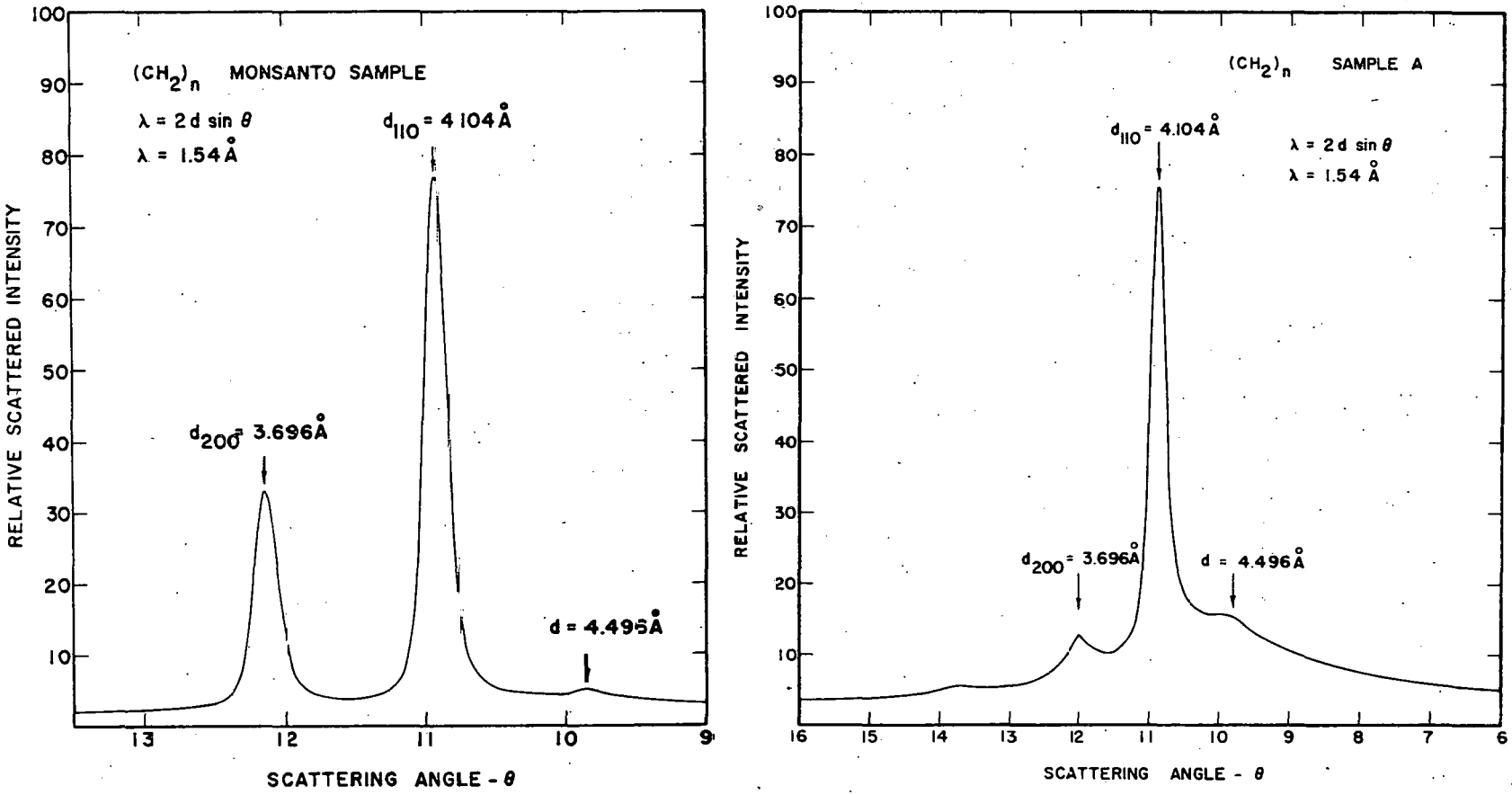

Fig. 31--X-ray scattering patterns from two different specimens of polyethylene used in neutron scattering experiments. Sample A is a low density (0.920 g/cc) sample, while the Monsanto sample is very dense (0.963 g/cc) and highly crystalline

APPENDIX II

SELECTED BIBLIOGRAPHY

Papers and Reports on Differential Neutron Thermalization under Contract AT(04-3)-167, P.A. 10, and Related General Atomic Programs - (1959, and 1960).

Whittemore, L. L., Annual Summary Reports on Differential Neutron Thermalization under Contract AT(04-3)-167, P.A. 10, USAEC reports GA-2503 (1961), GA-3409 (1962), GA-4434 (1963), and GA-5554 (1964).

Pelah, I., W. L. Whittemore, and A. W. McReynolds, "Energy Distribution of Neutrons Scattered by Liquid Lead," Phys. Rev. 113, 767 (1959).

Whittemore, W. L., and A. W. McReynolds, "Effects of Chemical Binding on the Neutron Cross Section of Hydrogen, Phys. Rev. 113, 806, (1959).

McReynolds, A. W., and W. L. Whittemore, "Slow Neutron Scattering by Hydrogen," presented at American Physical Society meeting, Washington, April 30 -- May 2, 1959. Bull. Am. Phys. Soc. 4, 246 (1959).

Whittemore, W. L., A. W. McReynolds and I. Pelah, "A Neutron Time-of-Flight Study of the Einstein Energy of Several Metal Hydrides," presented at American Physical Society meeting, Washington, April 30 - May 2, 1959. Bull. Am. Phys. Soc. 4, 246 (1959).

Parks, D. E., "Neutron Thermalization in Graphite," General Atomic report GAMD-742, April 1959.

Parks, D. E., D. H. Perkel, and F. N. Wikner, "Thermal-Neutron Spectra in Polycrystalline Graphite," presented at ANS meeting, Gatlinburg, Tennessee, June 15-17, 1959. Trans. Am. Nucl. Soc. 2, 244 (1959).

Nelkin, M. S., "Neutron Thermalization in Water," General Atomic report GA-1180, January, 1960.

Whittemore, W. L., and A. W. McReynolds, "Measurement of Neutron Transport Cross Section by Crystal Spectrometer Techniques," presented at American Physical Society meeting, New York, January 27-30, 1960. Bull. Am. Phys. Soc. 5, 17 (1960).

Nelkin, M. S., "The Scattering of Slow Neutrons by Water," Phys. Rev. 119, 741 (1960).

Nelkin, M. S., and D. E. Parks, "The Effects of Chemical Binding on Nuclear Recoil," Phys. Rev. 119, 1060 (1960).

McReynolds, A. W., and W. L. Whittemore, "Linac Measurements of Hydrogen Bonding Effects on Neutron Thermal Inelastic Scattering," Conference on Neutron Diffraction in Relation to Magnetism and Chemical Binding, Gatlinburg, Tennessee, April, 1960.

McReynolds, A. W., and W. L. Whittemore, "Inelastic Scattering of Neutrons from Very Cold Materials," presented at the International Atomic Energy Agency Conference on Inelastic Scattering of Neutrons in Solids and Liquids, Vienna, October 11-14, 1960. Published in Inelastic Scattering of Neutrons in Solids and Liquids, (IAEA, Vienna, 1961) pp 421 ff.

Whittemore, W. L., and A. W. McReynolds, "Inelastic Scattering of Thermal Neutrons Produced by an Accelerator," presented at the International Atomic Energy Agency Conference on Inelastic Scattering of Neutrons in Solids and Liquids, Vienna, October 11-14, 1960. Published in Inelastic Scattering of Neutrons in Solids and Liquids, (IAEA, Vienna, 1961) pp 511 ff.

Whittemore, W. L., "A Small Neutron Beam Chopper," General Atomic report GAMD-1961, January 18, 1961.

McReynolds, A. W., and W. L. Whittemore, "Structure and Dynamics of Liquid Hydrogen by Neutron Scattering," presented at American Physical Society Meeting, Washington, April, 1961. Bull. Am. Phys. Soc. 6, 262, (1961).

Whittemore, W. L., and A. W. McReynolds, "Neutron Scattering by Low-Temperature H_2O," presented at American Physical Society Meeting, Washington, April, 1961. Bull. Am. Phys. Soc. 6, 262, 1961.

McReynolds, A. W., and W. L. Whittemore, "Structure and Dynamics of Liquid Hydrogen by Neutron Scattering," presented at the International Atomic Energy Agency Conference on Inelastic Scattering of Neutrons in Solids and Liquids, Chalk River, September 10-14, 1962. In Inelastic Scattering of Neutrons in Solids and Liquids, (IAEA, Vienna, 1963) Vol. I, pp 263 ff.

Whittemore, W. L., and H. R. Danner, "Neutron Interactions in Liquid Para- and Ortho-Hydrogen," presented at the International Atomic Energy Agency Conference on Inelastic Scattering of Neutrons in Solids and Liquids, Chalk River, September 10-14, 1962. Published in Inelastic Scattering of Neutrons in Solids and Liquids, (IAEA, Vienna, 1963) Vol. I, pp 273 ff.

Whittemore, W. L., "Inelastic Neutron Scattering in Liquid Methane and Liquid Parahydrogen." Nucl. Sci. and Eng. 18, 182 (1964).

Whittemore, W. L., "Neutron Interactions in Zirconium Hydride," General Atomic report GA-4490 (Rev.) January, 1964.

Hom, A. K., and W. L. Whittemore, "Neutron Velocity Selector for an Electron Linac," presented at the American Physical Society Meeting in Pasadena, December, 1963.

Whittemore, W. L., and A. K. Hom, "Neutron Interactions in Zirconium Hydride," presented at the American Physical Society Meeting in Pasadena, December, 1963.

Whittemore, W. L., "Evidence of Anharmonic Motion of Hydrogen in Zirconium Hydride," presented at the American Physical Society Meeting in New York City, January, 1964.

Whittemore, W. L., "The Nature of Hydrogen Motion in ZrH Determined from an Experimental Neutron Study of Large Bound Energy Levels," IAEA Symposium on Inelastic Scattering of Neutrons in Solids and Liquids, GA-5744, October 7, 1964. To be published in IAEA Proceedings.

Whittemore, W. L., "Experimental Determination of Neutron Inelastic Scattering in Polyethylene" and "Inelastic Scattering of Neutrons by Reactor Type Graphite" to be presented at a Symposium on the Inelastic Scattering of Neutrons by Condensed Systems, Brookhaven National Laboratory, September 1965.

Whittemore, W. L., "Inelastic Scattering of Neutrons by Polyethylene" and "Neutron Scattering by Graphite", to be presented at a National Topical Meeting of the American Nuclear Society in San Diego, February 1966.

Whittemore, W. L., "Scattering of Neutrons by Polyethylene", General Atomic report GA-6456, June 1965. To be published in Nucl. Sci. and Eng.